

UNCLASSIFIED

AD NUMBER
AD248951
NEW LIMITATION CHANGE
TO Approved for public release, distribution unlimited
FROM Distribution: Further dissemination only as directed by Wright Air Development Division, Air Research and Development Command, USAF, Wright-Patterson Air Force Base, OH 45433; 30 Sep 1959 or higher DoD authority.
AUTHORITY
ASD, USAF ltr, 6 Aug 1974.

THIS PAGE IS UNCLASSIFIED

UNCLASSIFIED

This Document
Reproduced From
Best Available Copy

AD 248 951L

*Reproduced
by the*

ARMED SERVICES TECHNICAL INFORMATION AGENCY
ARLINGTON HALL STATION
ARLINGTON 12, VIRGINIA



UNCLASSIFIED

NOTICE: When government or other drawings, specifications or other data are used for any purpose other than in connection with a definitely related government procurement operation, the U. S. Government thereby incurs no responsibility, nor any obligation whatsoever; and the fact that the Government may have formulated, furnished, or in any way supplied the said drawings, specifications, or other data is not to be regarded by implication or otherwise as in any manner licensing the holder or any other person or corporation, or conveying any rights or permission to manufacture, use or sell any patented invention that may in any way be related thereto.

WADC TECHNICAL REPORT 58-284
PART III

PERFORMANCE OF TRAILING AERODYNAMIC
DECELERATORS AT HIGH DYNAMIC PRESSURES

PART III
WIND TUNNEL TESTING OF RIGID AND FLEXIBLE
PARACHUTE MODELS

B. A. Engstrom
R. A. Meyer

Cook Research Laboratories
A Division of Cook Electric Company
Chicago, Illinois

1959

This report is not to be announced or distributed automatically
in accordance with AFR 205-43A, paragraph 6d

WRIGHT AIR DEVELOPMENT DIVISION

NOX

CATALOGED BY ASTIA
AD NO. 248 951

WADC TECHNICAL REPORT 58-284
PART III

PERFORMANCE OF TRAILING AERODYNAMIC DECCELERATORS AT HIGH DYNAMIC PRESSURES

PART III

WIND TUNNEL TESTING OF RIGID AND FLEXIBLE PARACHUTE MODELS

B. A. Engstrom
R. A. Meyer

Cook Research Laboratories
A Division of Cook Electric Company
Chicago, Illinois

1959

Parachute Branch
Aeronautical Accessories Laboratory
Contract No. AF 33(616)-5507
Project No. 6065-61525

WRIGHT AIR DEVELOPMENT DIVISION
AIR RESEARCH AND DEVELOPMENT COMMAND
UNITED STATES AIR FORCE
WRIGHT-PATTERSON AIR FORCE BASE, OHIO

FOREWORD

This report was prepared by personnel of the Cook Research Laboratories, a division of the Cook Electric Company, Chicago, Illinois, in compliance with Item VII, Part I of Contract No. AF 33(616)-5507. The project was initiated by the Parachute Branch, Aeronautical Accessories Laboratory, Wright Air Development Center, with Rudi Berndt as project officer. The work at the Cook Research Laboratories on Project P-1031A was under the supervision of Dr. J. R. Downing, Director; R. O. Fredette, Associate Director; Dr. H. V. Hawkins, Assistant Director; and B. A. Engstrom, Project Engineer. The work was initiated on 1 March 1958 and completed 28 February 1959.

Staff members who contributed to the project include, L. J. Lorenz, Executive Engineer; F. A. Ruprecht, Superintendent, Parachute Department; W. H. Henricks, Senior Engineer; and A. J. Alexander, Designer.

Acknowledgment is made of the excellent cooperation of personnel of the NASA at the Unitary Plan Wind Tunnel, Langley Research Center, Virginia, in providing facilities and conducting tests. Those persons who were particularly helpful included: H. A. Wilson, J. D. Maynard, and J. Pressnell.

ABSTRACT

This report presents the results of the third phase of a continuing study of the Performance of Trailing Aerodynamic Decelerators at High Dynamic Pressures and covers experiments performed in the Unitary Plan Wind Tunnel at the Langley Research Center, Virginia. The work was also a continuation of the effort initiated under Contract No. AF 33(616)-3346. The major results of the Phase III test program were as follows: (1) solid metal canopies without suspension lines which were properly vented exhibited stable flow at all times regardless of changes in porosity, Mach number, dynamic pressure, and various other parameters; (2) the addition of suspension lines to the solid canopies caused unstable flow to exist at all times; (3) reducing the number of suspension lines or adding flow stabilizers did not improve flow patterns; (4) fabric canopies behaved poorly in general and appeared to be somewhat dependent upon the location of a conical interline shock wave; (5) a definite improvement was noted when the number of gores was increased; (6) average drag coefficient was a function of average inflated area ratio; and (7) shaped gores improved behavior somewhat, the 45° conical ribbon giving the most stable performance of all fabric configurations tested.

PUBLICATION REVIEW

This report has been reviewed and is approved.

For the Commander:



WARREN P. SHEPARDSON
Chief, Parachute Branch
Aeronautical Accessories Laboratory

TABLE OF CONTENTS

<u>Section</u>		<u>Page</u>
I	INTRODUCTION	1
	A. General	1
	B. Background	1
	C. Scope	2
II	TEST METHODS AND EQUIPMENT	4
	A. Test Facility	4
	B. Test Models and Equipment	4
	1. General	4
	2. Rigid Parachute Models	9
	3. Fabric Parachute Models	10
III	TEST RESULTS	12
	A. General	12
	B. Canopy Alone	12
	C. Canopy with Lines	14
	D. Fabric Canopies	18
	1. Porosity Variation	18
	2. Three Parachute Cluster	21
	3. Test No. 5, FIST Ribbon with Pulled-in Crown	21
	4. Horizontal Ribbon Space Ratio Variation	23
	5. Conical Ribbon	26
	E. Discussion of Results	28
IV	GENERAL CONCLUSIONS	30
APPENDICES		
I	RIGID PARACHUTE MODEL DESIGN	32

TABLE OF CONTENTS (cont'd)

<u>Section</u>		<u>Page</u>
	APPENDICES (cont'd)	
	A. General	32
	B. Stress Analysis	32
	1. Yoke Support	33
	2. Canopy	34
	3. Suspension Lines	37
II	FABRIC MODEL PARACHUTE DESIGN	39
	A. Introduction	39
	B. Parachute Design	39
III	STRESS ANALYSIS OF THE FABRIC PARACHUTE MOUNTING AND DEPLOYMENT SYSTEM	44
	A. General	44
	B. Deployment Mechanism	44
	1. Attachment Lug	45
	2. Deployment Piston	46
	3. Stop Pins	47
	4. Combustion Chamber	47
	5. Parachute Chamber	48

LIST OF ILLUSTRATIONS

<u>Figure</u>		<u>Page</u>
1	Typical Views of Rigid Parachute Model Mounted in Langley 4 x 4 Wind Tunnel	5
2	Support System for Fabric Parachute Testing in the Langley 4 x 4 Tunnel	6
3	Typical Rigid Parachute Model Assembled to Yoke Type Sting	9
4	Several Rigid Parachute Model Configurations	10
5	Typical Behavior of Several Rigid Parachute Canopies without Suspension Lines	13
6	Typical Behavior of a Rigid Canopy of 45% Porosity and with 24 Suspension Lines	15
7	Typical Behavior of a Rigid Canopy of 20% Porosity and with 24 Suspension Lines (From Ref. 1)	16
8	Typical Behavior of a Rigid Canopy of 45% Porosity with 12 Suspension Lines	17
9	Typical Behavior of a Rigid Canopy of 45% Porosity with 6 Suspension Lines	19
10	Typical Behavior of a Rigid Parachute of 45% Canopy with 6 Suspension Lines	20
11	Typical Fabric Parachute Behavior at Mach 1.9, Cluster and Pulled-in Vent	22
12	Horizontal Ribbon Ratio vs. Drag Coefficient and Area Ratio for 16 Gore Model Parachutes at Mach 1.9	24
13	Typical Fabric Parachute Behavior at Mach 1.9, Ribbon to Space Ratio Variation	25
14	Typical Fabric Parachute Behavior at Mach 1.9, Conical Ribbon	27

LIST OF ILLUSTRATIONS (cont'd)

<u>Figure</u>		<u>Page</u>
15	Typical Shock Patterns of Several Fabric Canopies at Mach 1.9	29
16	Typical Gore Layout for 8 Gore FIST Ribbon Parachutes	41
17	Typical Gore Layout for 16 Gore FIST and Conical Ribbon Parachutes	42

LIST OF TABLES

<u>Table</u>		<u>Page</u>
1	Phase III Test Schedule	3
2	Summary of Test Configurations, Test Conditions, and Observations. Test Programs in Unitary Plan Wind Tunnel, Langley Research Center with Rigid Parachute Models	7
3	Fabric Parachute Models	8
4	Physical Details of Ribbon Model Parachutes	43

SECTION I

INTRODUCTION

A. General

This report represents Part III of a continuing study of the Performance of Trailing Aerodynamic Decelerators at High Dynamic Pressures under Contract No. AF 33(616)-5507. Parts I and II of this series reported on the progress made with the free-flight test vehicle, Cree, during Phases I and II of the subject program. Concurrently with the free-flight testing of Phase II a wind-tunnel study program, Phase III, was conducted. The results of Phase III are discussed in this report.

B. Background

A study program of the nature and scope outlined in the subject contract requires the expenditure of considerable effort both in time and equipment on each free-flight test mission. Consequently, the items being tested should be of such a design that a reasonable assurance exists that the item will function in a satisfactory manner under a given set of test conditions. Investigations into new designs of drag devices with free-flight vehicles such as the Cree missile would be extremely costly because of the vast number of tests which must be conducted in any such developmental program.

The use of wind tunnels for research work of this nature allows a high rate of testing while at the same time permitting selection of a wide variety of test conditions and test models. After a workable design has been developed in an initial wind-tunnel phase the drag device or parachute can be proof-tested as a full-scale device under the actual test conditions desired by utilizing free-flight test vehicles. Thus, the use of wind tunnels for preliminary testing results in a much more orderly approach to the development of aerodynamic decelerators.

Such a basic wind-tunnel investigation was initiated under Contract No. AF 33(616)-3346, the results of which were reported in Reference 1, "Wind Tunnel Investigation of Conventional Types of Parachute Canopies in Supersonic Flow". In this program, both fabric and solid metal canopies were tested. The tests of fabric parachutes were conducted at the NASA Unitary Plan Wind Tunnel at the Lewis Research Center, Cleveland, Ohio, while the rigid models were tested at the Langley facilities of the NASA. Tests of fabric parachutes in the Lewis phase indicated the following major results: (1) violent canopy breathing or pulsing tendencies and associated reduced inflation and drag characteristics; (2) shock pattern fluctuations which were

complicated by interaction effects due to material flexibility; and (3) the failure of ribbons due to violent oscillation of the ribbon fabric. In order to establish the cause of pulsation as evidenced in the Lewis program, a scaled rigid model was utilized in the Langley phase so as to eliminate the interaction effects of flexibility. Although flexibility effects were eliminated by the use of a rigid model, the fluctuations and discontinuities of the shock patterns were still in evidence. This condition was attributed partly to choking of the flow through the canopy and also the interaction of the shock fronts due to choking and disturbances from the confluence point of the lines.

C. Scope

The results of the previous program (Reference 1) indicated the need for much more development work. The occurrence of shock pattern discontinuities and unstable flow characteristics during the preceding program indicated that utilization of higher porosity, vented canopies was a logical approach for future test programs. Accordingly, rigid parachute models incorporating these features and such others worthy of investigation were fabricated and subjected to test. In addition, various small fabric parachute models and a cluster of three ribbon parachutes were investigated. Tests were conducted over a range of Mach numbers of from 1.70 to 3.50. Dynamic pressures were varied between 100 and 540 psf. The test program was accomplished in two phases, one involving solid metal canopies of various porosities and both with and without suspension line, and the second involving fabric parachutes of various configurations. The entire test program is outlined in Table 1.

TABLE 1

PHASE III TEST SCHEDULE

Phase and Type	Test Dates	Test No.	Porosity %	Suspension Lines	Other Details	Mach No.	Dynamic Pressure
I-a Rigid	28 April to 1 May 1958	1	45	24-2D	-	2.30	-
		2	45	24-2D	-	2.65	-
I-b Rigid	June 1958	1	45	None		3.50	150
		2	45	None		3.00	250
		3	45	None		2.30	190
		4	45	24-1D		3.50	160
		5	45	24-1D		3.00	250
		6	45	24-1D		2.30	190
		7	45	12-1D		3.50	160
		8	45	12-1D		3.00	250
		9	45	12-1D		2.30	190
		10	45	24-2D		3.5	160
		11	45	24-2D		3.0	-
		12	36.5	None		1.70	540
		13	36.5	None	$\alpha = 5^\circ$	1.70	540
		14	35.0	None		1.70	300
		15	35.0	None	$\alpha = 5^\circ$	1.70	300
I-c Rigid	Sept. 1958	1	45.0	12-1D		1.77	290
		2	45.0	12-1D		2.17	240
		3	45.0	12-1D		2.76	155
		4	45.0	6-1D		1.77	290
		5	45.0	6-1D		2.17	240
		6	45.0	6-1D		2.76	155
		7	45.0	6-1D	$\alpha = 2^\circ$	2.76	155
		8	45.0	6-1D	Flow Stab.	2.76	155
		9	45.0	6-1D	Flow Stab.	2.76	100
		10	28.0	None		1.77	290
		11	28.0	None		2.17	240
		12	28.0	None		2.76	155
II Flexible	7-9 Jan. 1959	1	40.5	8-1D	Large vent	1.9	162.3
		2	33.8	8-1D	Large vent	1.9	155.06
		2a	33.8	8-1D	Large vent	2.135	144.9
		3	20.0	8-1D	-	1.9	165.5
		4	20.0	8-1D	Cluster	1.9	172.03
		5	20.0	8-1D	Pulled in vent	1.9	169.85
		6	29.03	16-1D	$R_{HR} = 1.50$	1.9	165.96
		7	24.96	16-1D	$R_{HR} = 0.586$	1.9	163.36
		8	28.5	16-1D	$R_{HR} = 1.145$	1.9	164.0
		9	28.5	16-1D	45° conical	1.9	160.72
		10	28.3	16-1D	30° conical	1.9	174.86
		10a	28.3	16-1D	30° conical	2.0	162.8

SECTION II

TEST METHODS AND EQUIPMENT

A. Test Facility

The test facility utilized for this program was the Unitary Plan Wind Tunnel located at the Langley Research Center of the NASA. This wind tunnel has two 4 ft x 4 ft test sections, each approximately 7 feet long; and, depending upon availability, both were used at various times during this program.

The low range test section (No. 1) has a design Mach number range of from 1.5 to 2.9 and is capable of stagnation pressure variations up to a maximum of approximately 60 psia. The high range test section (No. 2) has a design Mach number range from 2.3 to 5.0. Its maximum stagnation pressure is approximately 150 psia.

Each test section will permit variation of Mach number at any desired increment throughout its range while the tunnel is operating. Both stagnation pressure and stagnation temperature may be controlled independently if desired.

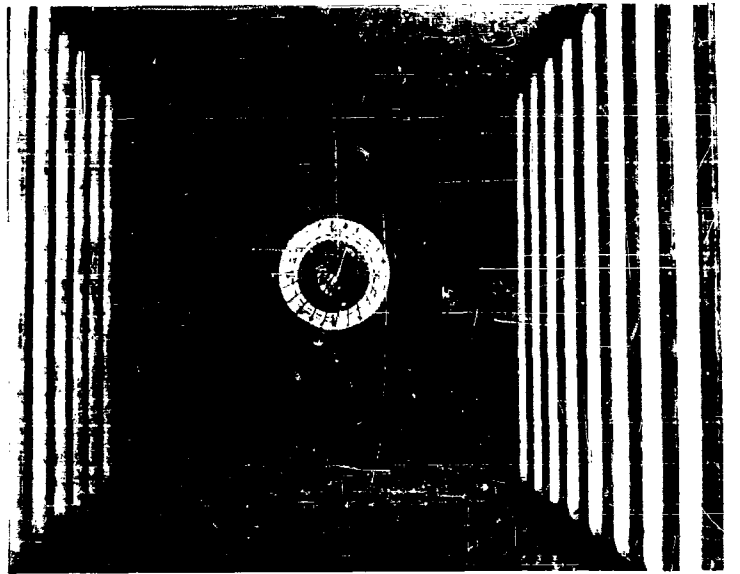
Each Schlieren window has a field of view of 59 in. x 48 in. The window is rectangular and made up of nine strips of optical plate glass, each 5-1/2 inches wide and separated from each other by 1-1/4 inches of supporting structure. This arrangement permits the attainment of a large field of view while retaining excellent optical qualities.

Only the low range (No. 1) test section was utilized for tests of the fabric parachutes. All tests were conducted at a Mach number of 1.9. At this Mach number, the parachute riser length was limited to 26 to 28 inches to prevent interference with shock wave reflections from the tunnel walls.

B. Test Models and Equipment

1. General

Both rigid and fabric parachute test models were utilized during the test program. Figure 1 shows two views of a typical rigid canopy mounted in the tunnel ready for testing. Figure 2 shows the sting and support structures utilized in testing fabric canopies. Tables 2 and 3 are summary tables which show physical characteristics, test conditions, and general observations for all configurations of both rigid and fabric types. Variations

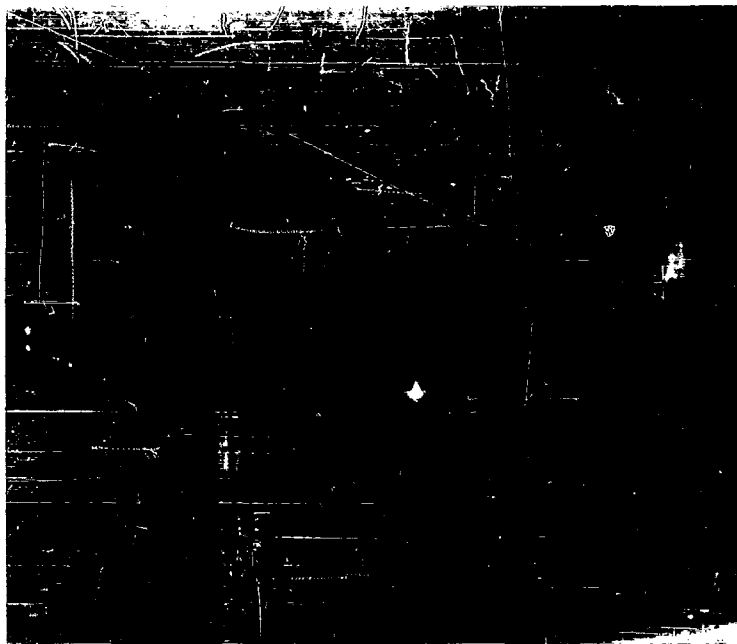


(a) Looking Downstream

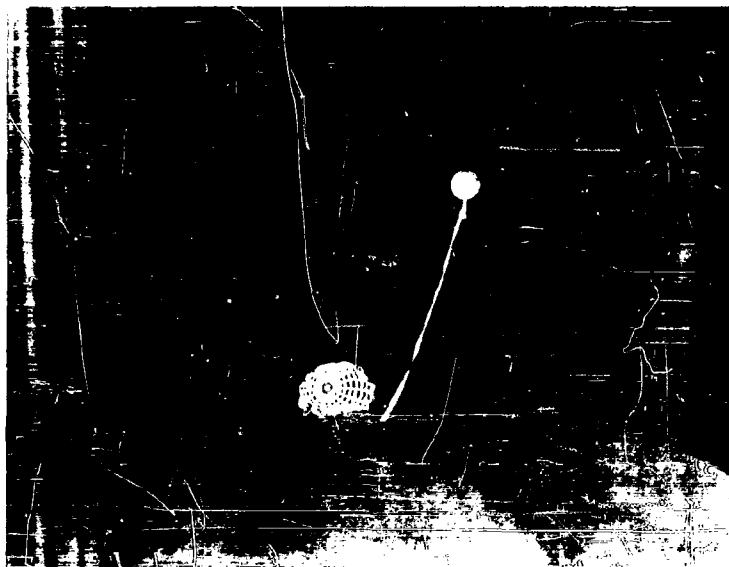


(b) Looking Upstream

Figure 1. Typical Views of Rigid Parachute Model Mounted in Langley 4 x 4 Wind Tunnel



(a) Looking Downstream



(b) Looking Upstream

Figure 2. Support System for Fabric Parachute Testing in the Langley 4 x 4 Tunnel

WADC TR 58-284
PART III

TABLE 2

SUMMARY OF TEST CONFIGURATIONS, TEST CONDITIONS, AND OBSERVATIONS.
TEST PROGRAMS IN UNITARY PLAN WIND TUNNEL, LANGLEY RESEARCH CENTER
WITH RIGID PARACHUTE MODELS

Configuration No.	Test Configuration	Configuration Characteristics				No. of Suspension Lines	Test Conditions and Observations				Observations and/or Remarks
		Constructed (D ₀) (in.)	Inflated (D ₁) (in.)	Total Porosity (% Total Porosity Area)	Vent Size & (% Total Porosity Area)	Ratio of Line Length to Constructed Diameter (L/D ₀)	Mach No. (M)	Dynamic Pressure (q) (psf)	Angle of Attack (α) (deg)	Camera Frame Speed (fr/sec)	
1 ^a	Canopy alone	12.0	8.0	20.0	No Vent	0	2.30	200	0	2160	Unsteady flow with canopy bending & violent rotary motion inside
							2.98	200	0	1440	Steady flow
							3.50	200	0	1920	Unsteady flow
							3.71	200	0	1800	Steady flow
2 ^a	Canopy alone	12.0	8.0	24.0	No Vent	0	3.00	200	0	1680	Unsteady flow
							3.04	200	0	1680	Steady flow
							3.35	150	1.0	2280	Unsteady flow
							3.60	125	0	1440	Steady flow
							3.60	150	0	2280	Unsteady flow apparently the result of increase in q (see preceding entry)
							3.70	140	0	1800	Steady flow
							3.90	115	0	1660	Steady flow
							3.90	115	4.0	1860	Steady flow 4° angle of attack had little effect
3 ^a	Canopy with lines	12.0	8.0	20.0	No Vent	1.0	1.57	200	0	1560	For all Mach numbers flow was unsteady - considerable shock wave fluctuation in all these cases
							1.87	200	0	1020	
							2.16	200	0	1500	
							2.30	200	0	480	
							2.98	200	0	960	
							3.71	200	0	480	
4 ^a	Canopy with lines	12.0	8.0	20.0	No Vent	2.0	3.20	100	0	2160	Bow wave relatively steady, considerable suspension line bending
							3.71	200	0	480	Bow wave relatively steady, no noticeable line bending
5	Canopy alone	12.0	8.0	28.0	Large (6.5%)	0	1.77	290	0	2640	Steady flow - little change w/ Mach No.
							2.17	240	0	1800	Steady flow
6	Canopy alone	12.0	8.0	35.0	Normal (1.1%)	0	2.76	155	0	960	Steady flow
							1.70	300	0	2160	Steady flow
7	Canopy alone	12.0	8.0	36.5	Large (16%)	0	1.70	300	5.0 (approx.)	1440	Steady flow 50° angle of attack had little effect on flow steadiness
							1.70	540	0	-	Steady flow
8	Canopy alone	12.0	8.0	45.0	Large (26%)	0	1.70	540	<5.0	-	Steady flow, angle of attack less than 3° had little effect
							2.30	190	0	1560	Steady flow
9	Canopy with lines	12.0	8.0	45.0	Large (26%)	1.0	3.00	250	0	1320	Steady flow
							3.50	150	0	-	Steady flow
							2.30	190	0	1440	Unsteady flow at all these Mach numbers - considerable shock wave fluctuation
10	Canopy with lines	12.0	8.0	45.0	Large (26%)	1.0	3.00	250	0	1440	Unsteady flow at all Mach numbers
							3.50	160	0	2040	
							2.30	190	0	1080	
							3.00	250	0	1800	
							3.50	160	0	1320	
11	Canopy with lines	12.0	8.0	45.0	Large (26%)	1.0	1.77	290	0	2640	
							2.17	240	0	960	
							2.76	155	0	2520	Unsteady flow - perhaps worse than Configuration No. 11
							2.76	155	2.0	1800	
11a	Canopy with lines	12.0	8.0	45.0	Large (26%)	1.0	2.76	155	0	1920	Flow stabilizers on lines - located approx. 4 inches from skirt of canopy
							2.76	100	0	2280	Unsteady flow, no apparent improvement due to stabilizers
12	Canopy with lines	12.0	8.0	45.0	Large (26%)	2.0	2.30	-	0	1500	Unsteady flow at all Mach numbers
							2.65	-	0	1500	
							3.00	-	0	-	
							3.50	160	0	1800	

^aResults of tests of these configurations were obtained during an earlier program at Langley and are included here for comparative purposes (see WADC TR 58-532 for discussion of results).

TABLE 3

FABRIC PARACHUTE MODELS

Configuration and Test No.	Test Configuration	Configuration Characteristics										Test Conditions and Observations						
		Diameter (inches)			Geometric Porosity (P) of fabric (in. per sq. ft.)	Number of Gores	Ratio of Line Length to Constructed Diameter (L/D _c)	Vent Size and Porosity	Ratio of Space between Ribs, (b/B _{rig})	Additional Features and/or Remarks	Mach No. (M)	Dynamic Pressure (q) (psf)	Drag Force (lb)	Drag Coefficient (C _D)	Area Ratio (A _p /A)	Corrected Drag* Coefficient C _D (corr)	Remarks	
		Constructed (D _c)	Nominal (D _N)	Inflated (D _i)														
1	FIST Ribbon Parachute (No. 780)	12.0	11.40	7.6	102.0	8	1.0	Large (14%)	0.507	Porosity Variation Model 26 to 28 in. Riser	1.900	162.30	12.975	0.1130	0.241	0.209	Poor performance. Unstable with considerable bristling	
2	FIST Ribbon Parachute (No. 779)	12.0	11.40	7.6	102.0	8	1.0	Large (15%)	0.507	Porosity Variation Model 26 to 28 in. Riser	1.900 2.135	155.06 144.90	10.848 9.359	0.0970 0.0910	0.204 0.141	0.212 0.288	Slightly steadier than No. 1 Still not very good	
3	FIST Ribbon Parachute (No. 777)	12.0	11.40	7.6	102.0	8	1.0	Normal (1%)	0.507	Penalty Variation Model 26 to 28 in. Riser	1.900	165.50	12.137	0.1050	0.254	0.184	Better than No. 1 and No. 2. Interline shock wave very unstable	
4	Cluster of 3 FIST Ribbon Parachutes (Nos. 78 and 782) (individual parachute characteristics given)	6.5	6.15	4.1	27.8 (89.4 for cluster)	8	1.0	Normal (1%)	0.615	Individual Parachute of 3-Cluster Cluster (5% of 1 'chutes - 89.4 in. 2) 26 to 28 in. Riser	1.900	172.03	-	-	-	-	Heavy breathing and violent oscillation. Very unsatisfactory	
5	FIST Ribbon Parachute with Pulled-in Crown (No. 786)	12.0	11.40	7.6	102.0	8	1.0	Normal (1%)	0.507	Canopy Crown Pulled into approx. 50% of inflated Depth by Central Line 26 to 28 in. Riser	1.900	169.75	13.455	0.1817	0.281	0.278	Better inflation. Numerous shocks off lines. Top of canopy quite flat. Deep scallops in skirt	
6	FIST Ribbon Parachute b/B _{rig} = 1.3 (No. 17862)	10.0	9.89	6.4	72.0	16	1.0	Normal (1%)	1.500	Space Ratio (b/B _{rig}) variation Model 26 to 28 in. Riser	1.900	165.56	24.035	0.2507	0.325	0.397	Much better inflation. Shock pattern steadier	
7	FIST Ribbon Parachute b/B _{rig} = 0.586 (No. 17869)	12.0	11.90	7.3	112.0	16	1.0	Normal (1%)	0.586	Space Ratio (b/B _{rig}) variation Model 26 to 28 in. Riser	1.900	163.36	27.438	0.2160	0.241	0.399	Best so far. Quite steady with slight breathing. Interline shock wave oscillating	
8	FIST Ribbon Parachute b/B _{rig} = 1.145 (No. 17881)	11.2	11.10	7.4	96.8	16	1.0	Normal (1%)	1.145	Space Ratio (b/B _{rig}) variation Model 26 to 28 in. Riser	1.900	164.03	28.289	0.2570	0.298	0.384	Not as good as No. 7. More breathing and more oscillation of interline shock	
9	45° Conical Ribbon Parachute (No. 17911)	11.7	9.77	-	75.0	16	1.0	Normal (1%)	1.050	45° Conical Ribbon Parachute DCP = 9.26 in. 26 to 28 in. Riser	1.900	160.72	18.719	0.2240	0.326	0.305	Best so far. Not much breathing or oscillation. Shock pattern quite steady. Interline shock oscillating slightly.	
10	30° Conical Ribbon Parachute (No. 17899)	12.0	11.57	-	95.7	16	1.0	Normal (1%)	0.813	30° Conical Ribbon Parachute DCP = 10.4 in. 26 to 28 in. Riser	1.900 2.000	174.86 162.80	28.289 26.375	0.2421 0.2420	0.266 -	0.405 -	Not as good as No. 9. More breathing and oscillation	

*The values of C_D(corr) were obtained by assuming the parachute canopy to be fully inflated and that the drag coefficient would increase linearly with increase in area ratio.

in geometric porosity and size of vent were considered in addition to changes in length and number of suspension lines. The pertinent characteristics and results of configurations tested previously and reported on in Reference 1 are included in Table 2 for comparative purposes.

2. Rigid Parachute Models

Since the results of Reference 1 had indicated that models with vents and increased porosity were desirable, the mounting system was altered to permit a vent in the crown of the canopy.

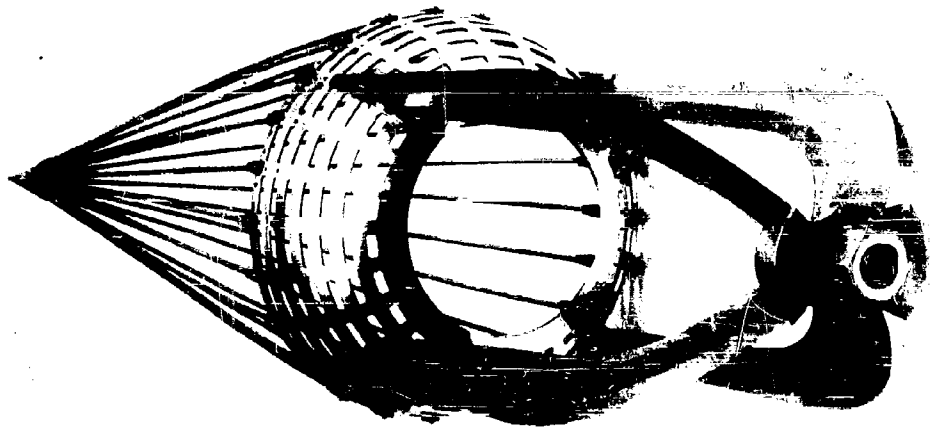


Figure 3. Typical Rigid Parachute Model Assembled to Yoke Type Sting

Figure 3 shows the yoke type mounting fixture which was devised to allow the adaptation to the present tunnel sting and still permit airflow through the crown of the canopy.

The stainless steel rigid models were constructed to the same general specifications as the 20 percent porosity model of Reference 1 but differed in the amount of porosity and in the addition of the vents which were provided. Three large-vent canopies of 28, 36.5, and 45 percent porosity, respectively, and a normal vent canopy of 35 percent porosity were fabricated for test purposes. Several of these canopies with various

suspension line arrangements are shown in Figure 4. Also shown are the flow stabilizer devices which were considered during the program to determine their effects on flow characteristics.

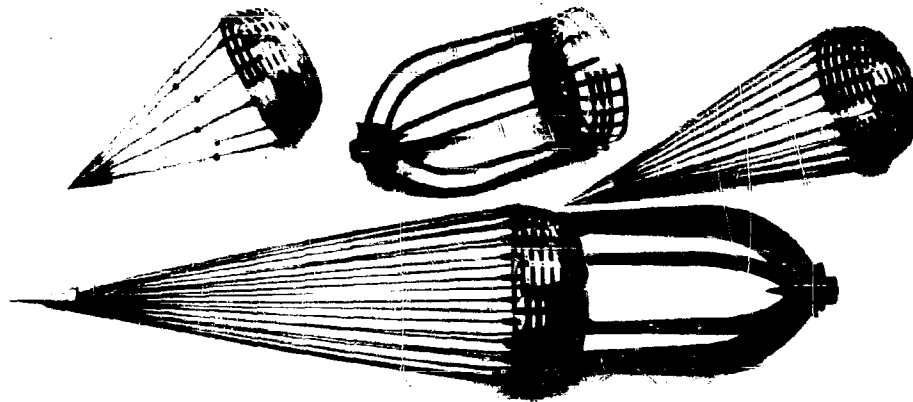


Figure 4. Several Rigid Parachute Model Configurations

Pertinent information relative to the design and stress analyses of the rigid models and the yoke type sting is presented in Appendix I.

3. Fabric Parachute Models

The fabric parachutes utilized in this investigation were designed so that effects of variations in porosity and in the ratio of the space-between-horizontal-ribbons to the horizontal-ribbon-width could be considered. These variations were considered in connection with conventional ribbon type parachutes. In addition, a cluster of three conventional ribbon parachutes and two conical ribbon parachutes were designed and constructed for test purposes.

The design details of all fabric parachutes are given in Appendix II. Pertinent figures are also included that illustrate these test configurations, and parachute details are tabulated. The dimensional characteristics and conditions under which the individual tests were conducted are given in Table 3. Drag coefficients obtained for these configurations are included in this table.

Consideration of the effects of porosity involved the use of three test parachutes with porosities of 40.5, 33.8, and 20.8 percent (Configuration Nos. 1, 2, and 3 in Table 3). Configurations 6, 7, and 8 were utilized to study the effects of variation in space ratio (b/B_{HR}).

A test of one fabric model (Configuration No. 5 of Table 3) involved a 20 percent porosity ribbon configuration with a pulled-in vent. This configuration was obtained by extending a central line from the midpoint or crossover point of the vent lines to the confluence point and sewing so that the crown of the parachute was pulled into the canopy to a point which was approximately 50 percent of the inflated depth.

Configuration 4 was a cluster of 3 ribbon parachutes. These parachutes were of conventional ribbon design with porosities of 20 percent and normal 1 percent vents.

The other two configurations (9 and 10) tested during this program were conical ribbon parachutes, i. e., the parachutes were designed to have cone angles of 45 and 30 degrees, respectively.

Mounting of the fabric parachute models in the low Mach number range test section required the use of a special support system which was designed and fabricated by these Laboratories. The design was based on a method suggested by cognizant wind-tunnel personnel of the Unitary Plan Wind Tunnel at the NASA Langley Research Center. A pictorial representation of this support system is presented in Figure 2. Details of the support system design including the parachute deployment mechanism are given in Appendix III.

SECTION III

TEST RESULTS

A. General

In general, test results were obtained in the form of visual and Schlieren film observations of the flow patterns about the models. For the most part, no force measurements were made except in the tests involving fabric parachutes. Consequently, the following will deal largely with a discussion of these observations as they pertain to specific configurations. Greater emphasis will naturally be placed, however, on those configurations which have shown favorable flow characteristics and for which some knowledge of drag forces has been obtained.

A tabulation of the various test configurations and their important characteristics is given in Tables 2 and 3. These two tables contain pertinent information for the rigid and fabric models, respectively.

The various test configurations are discussed in the following sections with regard to flow characteristics and, where measured, with respect to their drag-producing capabilities.

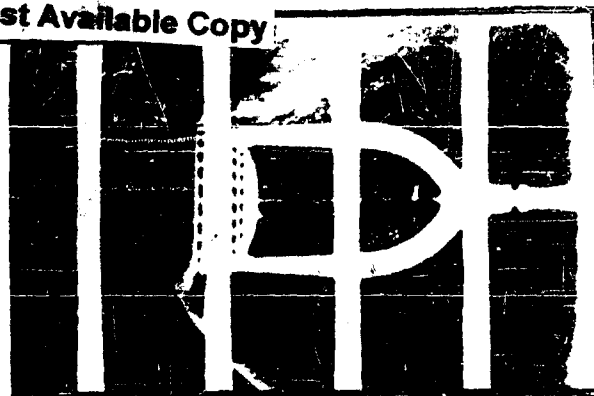
B. Canopy Alone

Canopy configurations without suspension lines were tested to investigate the flow characteristics of the canopies without the influence of suspension lines. Previous tests of 20 percent and 24 percent porosity canopies (Table 2) as reported in Reference 1 had indicated severe shock wave fluctuation and flow discontinuities which could be attributed to choking due to insufficient porosity and the lack of vents in the canopies. Preliminary efforts to improve flow characteristics were attempted during the program of Reference 1 by increasing the porosity of the original 20 percent porosity canopy to 24 percent. No significant improvement as a result of this small increase in porosity was evident, however. Thus, it was indicated (Reference 1) that higher porosity canopies with vents should be investigated.

As a result of the above, large-vent canopies with porosities of 28, 36.5 and 45 percent and a normal-vent canopy of 35 percent porosity were tested during this program. In general, the results of tests of the vented higher porosity canopies without lines were favorable with relatively steady shock patterns prevailing for all cases. Shock pattern photographs of these configurations at various Mach numbers are shown in Figure 5. These photographs are typical frame enlargements from the Schlieren high speed movie film.



(a) Porosity = 28%
Mach No. = 1.77
Dynamic Pressure = 290 P.S.F.



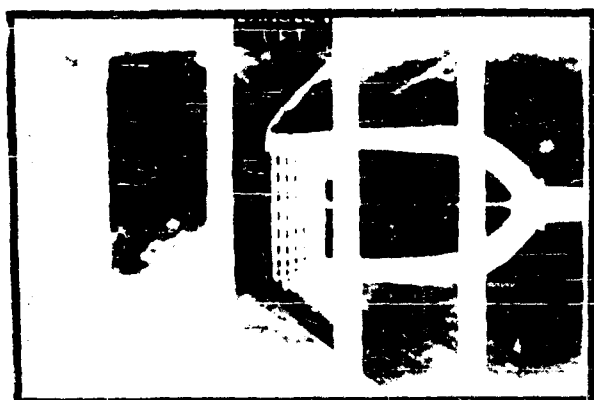
(b) Porosity = 28%
Mach No. = 2.17
Dynamic Pressure = 240 P.S.F.



(c) Porosity = 35%
Mach No. = 1.79
Dynamic Pressure = 300 P.S.F.
Angle of Attack = 0°



(d) Porosity = 35%
Mach No. = 1.70
Dynamic Pressure = 300 P.S.F.
Angle of Attack = 5°



(e) Porosity = 45%
Mach No. = 2.3
Dynamic Pressure = 190 P.S.F.



(f) Porosity = 45%
Mach No. = 3.50
Dynamic Pressure = 150 P.S.F.

Figure 5. Typical Behavior of Several Rigid Parachute Canopies without Suspension Lines

The 45 percent porosity canopy without suspension lines was tested at Mach numbers of 2.30, 3.00, and 3.50. The 36.5 percent large-vent canopy and the 35 percent normal-vent canopy were tested at a Mach number of 1.70. There was little or no oscillation of the shock waves during tests of the 45 percent porosity canopy without suspension lines and no evidence of canopy pulsing or breathing. A small angle of attack (5 degrees or less) at a test Mach number of 1.70 had little effect on the stable flow characteristics seen for both the large vent, 36.5 percent porosity canopy, and the normal vent, 35 percent porosity canopy.

The 28 percent canopy without suspension lines was tested at Mach numbers of 1.77, 2.17, and 2.76. In all cases, steady flow characteristics were seen. There was little apparent change with Mach number.

The shock formations observed during these tests of canopy without suspension lines are shown in Figure 5.

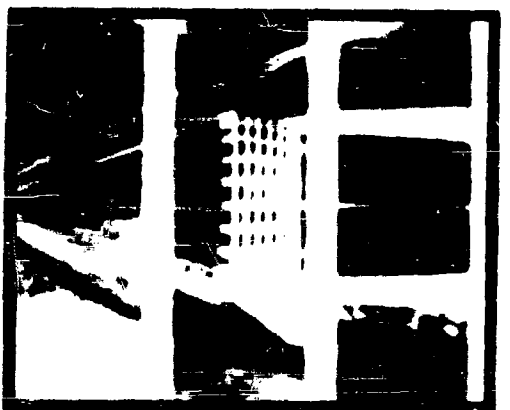
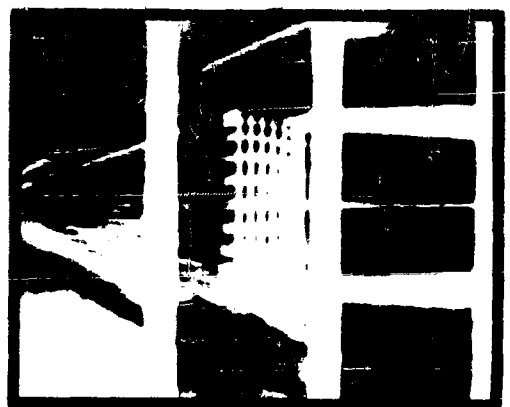
C. Canopy with Lines

The introduction of suspension lines to the metal canopies brought about a complete change in the flow patterns around the parachute. In general, the shock wave formations and the parachute behavior exhibited in these tests were similar to the results of the previous solid canopy tests conducted at the NASA Langley facility. Interaction between the shock front generated by the confluence point and the normal shock in front of the canopy caused violent changes in flow patterns and would no doubt have resulted in severe breathing and oscillation if flexibility had existed in the parachute configuration.

Figures 6 and 7 show both the results of this phase and those of Reference 1 for comparison. In both cases 24 suspension lines were used.

In an attempt to determine the extent of the effect of suspension lines, a series of tests was conducted wherein the number of suspension lines was reduced. Figure 8 shows a series of Schlieren frame enlargements taken during tests of a 45 percent canopy with 12 suspension lines over a range of Mach numbers. The general flow pattern with 12 suspension lines was more unstable than it was under the same conditions with 24 lines. There seemed to be more secondary shocks generated from the lines themselves and more movement in shock fronts than in the tests using 24 lines. As can be seen from Figure 8, the fluctuations increased with increase in Mach number.

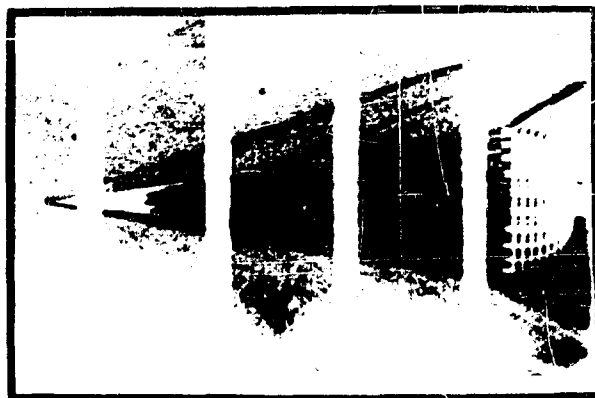
The investigation of the effect of suspension lines upon flow patterns was carried one step further. The number of lines was reduced to six and a series of tests run. Here again the shock patterns and fluctuations demonstrated no improvement over the cases where more suspension lines were



(a) Mach No. = 2.30
 Dynamic Pressure = 190 P.S.F.
 Film Speed = 1440 F.P.S.

(b) Mach No. = 3.50
 Dynamic Pressure = 160 P.S.F.
 Film Speed = 2040 F.P.S.

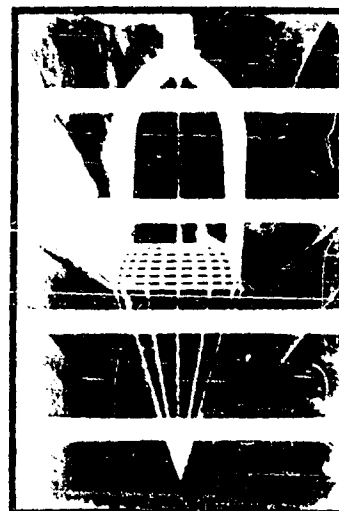
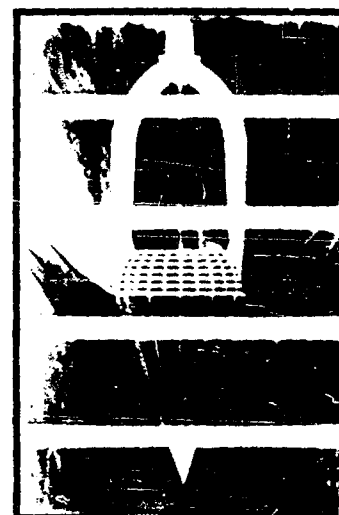
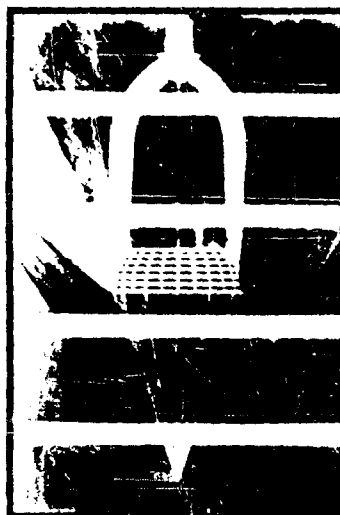
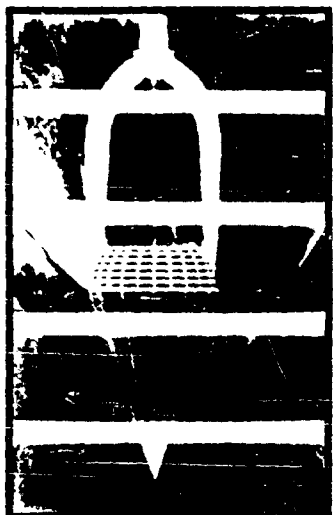
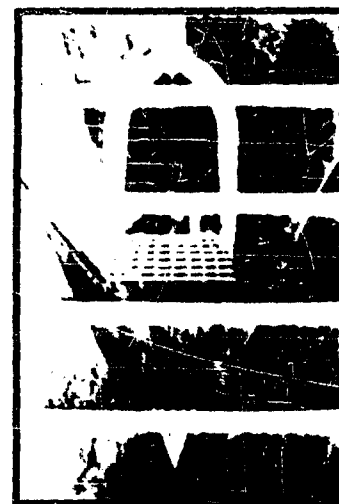
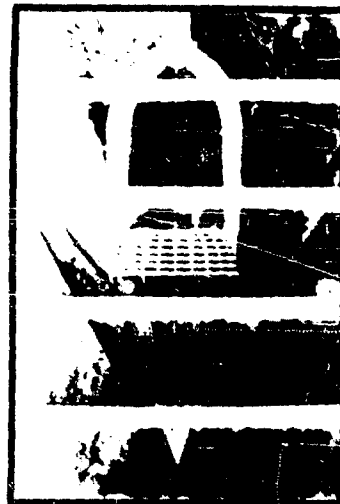
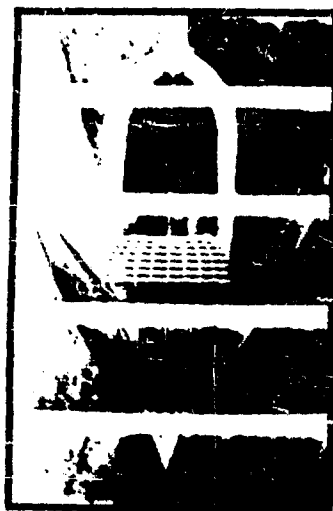
Figure 6. Typical Behavior of A Rigid Canopy of 45% Porosity and With 24 Suspension Lines



(a) Mach No. = 1.57
Dynamic Pressure = 200 P.S.F.
Suspension Lines = 24 x 1D.
Film Speed = 1560 F.P.S.

(b) Mach No. = 3.71
Dynamic Pressure = 200 P.S.F.
Suspension Lines = 24 x 2D
Film Speed = 480 F.P.S.

Figure 7. Typical Behavior of a Rigid Canopy of 20% Porosity and with 24 Suspension Lines (From Ref. 1)



(c) Mach No. = 2.76
Dynamic Pressure = 155 P.S.F.
Film Speed = 950 F.P.S.

(b) Mach No. = 2.17
Dynamic Pressure = 240 P.S.F.
Film Speed = 2040 F.P.S.

(a) Mach No. = 1.77
Dynamic Pressure = 290 P.S.F.
Film Speed = 2040 F.P.S.

Figure 8. Typical Behavior of A Rigid Canopy of 45% Porosity with 12 Suspension Lines

employed. Figures 9 and 10 show enlargements from Schlieren film for a number of test conditions. As the Mach number was increased the conditions became worse.

Introducing a 2 degree angle of attack did not bring about any appreciable change in the flow conditions (see Figure 10(b)). The addition of flow stabilizers on the suspension lines did introduce an additional shock front but had little effect as far as changing the over-all flow characteristics. This test is shown in Figure 10(c).

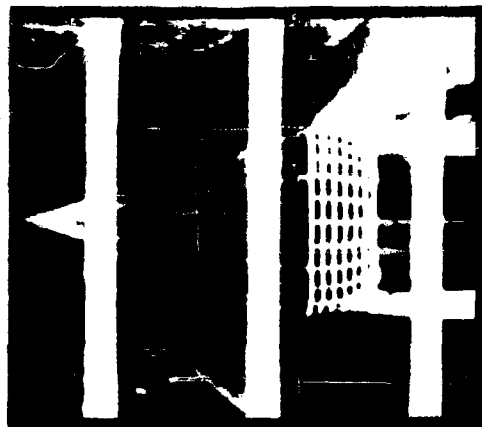
D. Fabric Canopies

1. Porosity Variation

The first group of fabric parachutes tested consisted of a series of three canopies similar in construction but presenting a variation in porosity. The porosities tested were 40.5, 33.8, and 20 percent. These parachutes had only eight gores and were assembled with suspension lines one diameter in length. The test Mach number was 1.9 in all cases, with one additional run at Mach 2.135 with the 33.8 percent porosity model. The 33.8 and 40.5 percent porosity canopies had large vents of 15 and 24 percent, respectively. The 20 percent porosity canopy had a normal 1 percent vent.

None of these parachutes performed satisfactorily. Drag force was measured and the drag coefficients of the various canopies calculated. In all three cases the drag coefficient, C_{D_0} , was very low averaging about 0.10. At the same time the parachute canopies exhibited serious underinflation. The area ratio, A_R , for the 40.5 percent canopy averaged 0.241 as compared with 0.445 for what is considered normal inflation. This particular parachute was therefore about 54 percent fully inflated. The other two tests of this series gave comparable results. The 33.8 percent canopy had an A_R equal to 0.204 and was therefore only 46 percent inflated. The 20 percent canopy had an A_R of 0.254 and was inflated 57 percent of normal.

Calculations made with the assumption that C_{D_0} would increase linearly with increase in area ratio proved that even when fully inflated the above parachutes would attain drag coefficients of only about 0.20.



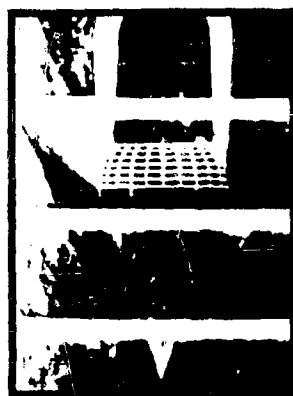
(a) Mach No. = 1.77
Dynamic Pressure = 290 P.S.F.
Film Speed = 3360 F.P.S.

(b) Mach No. = 2.17
Dynamic Pressure = 240 P.S.F.
Film Speed = 960 F.P.S.

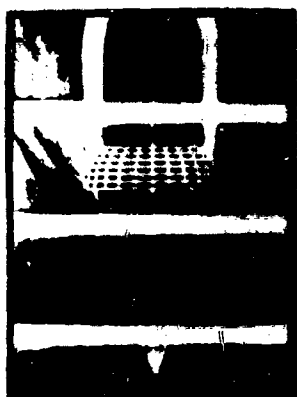
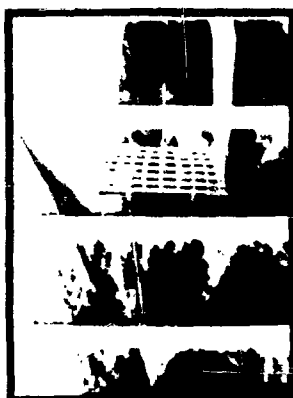
Figure 9. Typical Behavior of A Rigid Canopy of 45% Porosity
With 6 Suspension Lines



(a) Mach No. = 2.76
Dynamic Pressure = 155 P.S.F.
Angle of Attack = 0°
Film Speed = 2520 F.P.S.



(b) Mach No. = 2.76
Dynamic Pressure = 155 P.S.F.
Angle of Attack = 2°
Film Speed = 1800 F.P.S.



(c) Mach No. = 2.76
Dynamic Pressure = 155 P.S.F.
Angle of Attack = 0°
Film Speed = 1920 F.P.S.
Flow Stabilizers on Suspension Lines

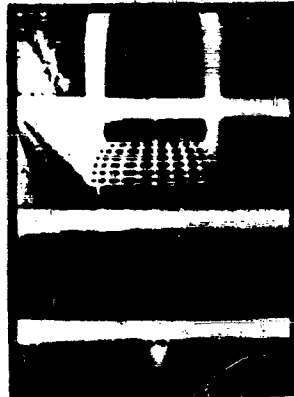
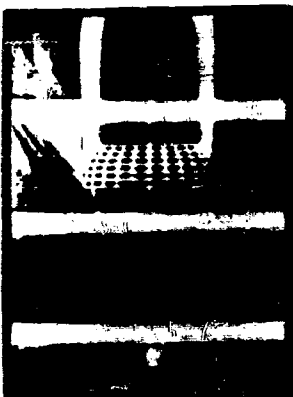


Figure 10. Typical Behavior of a Rigid Parachute of 45% Canopy
with 6 Suspension Lines

2. Three Parachute Cluster

In an attempt to avoid the column of low energy air existing in the wake behind the support body, a cluster of three parachutes was tried. This seemed like a logical approach since in a parachute cluster the canopies generally stand clear of each other and avoid the area directly behind the body. Therefore, three parachute canopies each having a nominal diameter of 6.15 inches were tried. These parachutes like the previous models also had eight gores and one diameter suspension line.

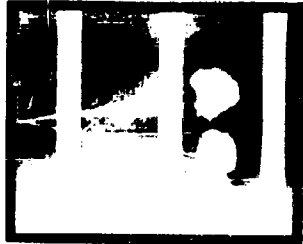
The test results were very poor. The canopies were underinflated with an average area ratio of only 0.172 or about 39 percent normal inflation. No drag data were obtained and therefore no drag coefficients could be calculated. Figure 11(a) shows a series of enlargements from Schlieren film and illustrates the violent oscillations and underinflation of the cluster parachutes.

3. Test No. 5, FIST Ribbon with Pulled-in Crown

In this test a standard FIST ribbon parachute of 20 percent porosity was modified by including a central line from the vent to the confluence point. This line was of a length such that when the canopy was inflated the vent would be pulled in about 50 percent of the inflated depth.

The Schlieren film data (see Figure 11(b)) indicated very erratic operation of the canopy with continuous breathing noted. Also, the parachute exhibited oscillating or coning motion throughout the test. The average drag coefficient was better than for the same parachute allowed to inflate normally being 0.181 as compared with 0.105. Also, the average area ratio was 0.291 while the standard canopy exhibited only 0.254. Thus, the parachute with the pulled-in vent demonstrated a higher inflated area ratio and a correspondingly higher drag coefficient.

However, the general behavior of the parachute was quite poor. The restraining influence of the central line kept the roof of the canopy relatively flat (see Figure 11(b)). The canopy oscillated considerably exhibiting very unstable characteristics. The skirt ribbon was deeply scalloped showing a lack of tension in the skirt region.



(a) Porosity = 20%
Cluster of 3, FIST Ribbon
Film Speed = 2270 F. P. S.
Dynamic Pressure = 172.03 P. S. F.



(b) Porosity = 20%
FIST Ribbon - Pulled in vent
Film Speed = 2240 F. P. S.
Dynamic Press = 169.85 P. S. F.

Figure 11. Typical Fabric Parachute
Behavior at Mach 1.9

4. Horizontal Ribbon Space Ratio Variation

There has been some evidence tending to indicate that one of the critical parameters in parachute design was the ratio of the width of the space between the horizontal ribbons to the width of the ribbon itself. A series of three tests was therefore executed involving parachute canopies of as nearly as possible the same size and porosity with horizontal ribbon ratios, R_{HR} , of 0.586, 1.145 and 1.500. In this series of tests parachutes having 16 gores were employed. Suspension line length was retained at one diameter and the test Mach number was unchanged at 1.9. The canopy porosities were maintained between 25 and 29 percent.

The test results were somewhat confusing. It has been expected that the highest value of R_{HR} would give the best results. In a sense this was true in that the average drag coefficient and area ratio for the three parachutes varied almost directly with increase in R_{HR} . For convenience these values are presented below.

Horizontal Ribbon Ratio R_{HR}	Drag Coefficient C_{Do}	Area Ratio A_R
0.586	0.216	0.241
1.145	0.257	0.298
1.500	0.290	0.325

These values are also plotted in Figure 12. Note that the plots of both C_{Do} and A_R increase almost linearly with increase in R_{HR} and that both curves have essentially the same slope.

Figure 13 shows a series of typical frame enlargements of the two extremes tested. From a behavior standpoint the canopy with the lowest ribbon ration, 0.586, performed the best. The intermediate canopy was not quite as good and the highest ribbon ratio canopy was the most unstable. From Figure 13(a) it can be seen that this configuration ($R_{BH} = 1.5$) oscillated violently and did considerable breathing. In spite of this instability, this parachute had the highest drag coefficient and area ratio of the three that were tested (see Figure 12).

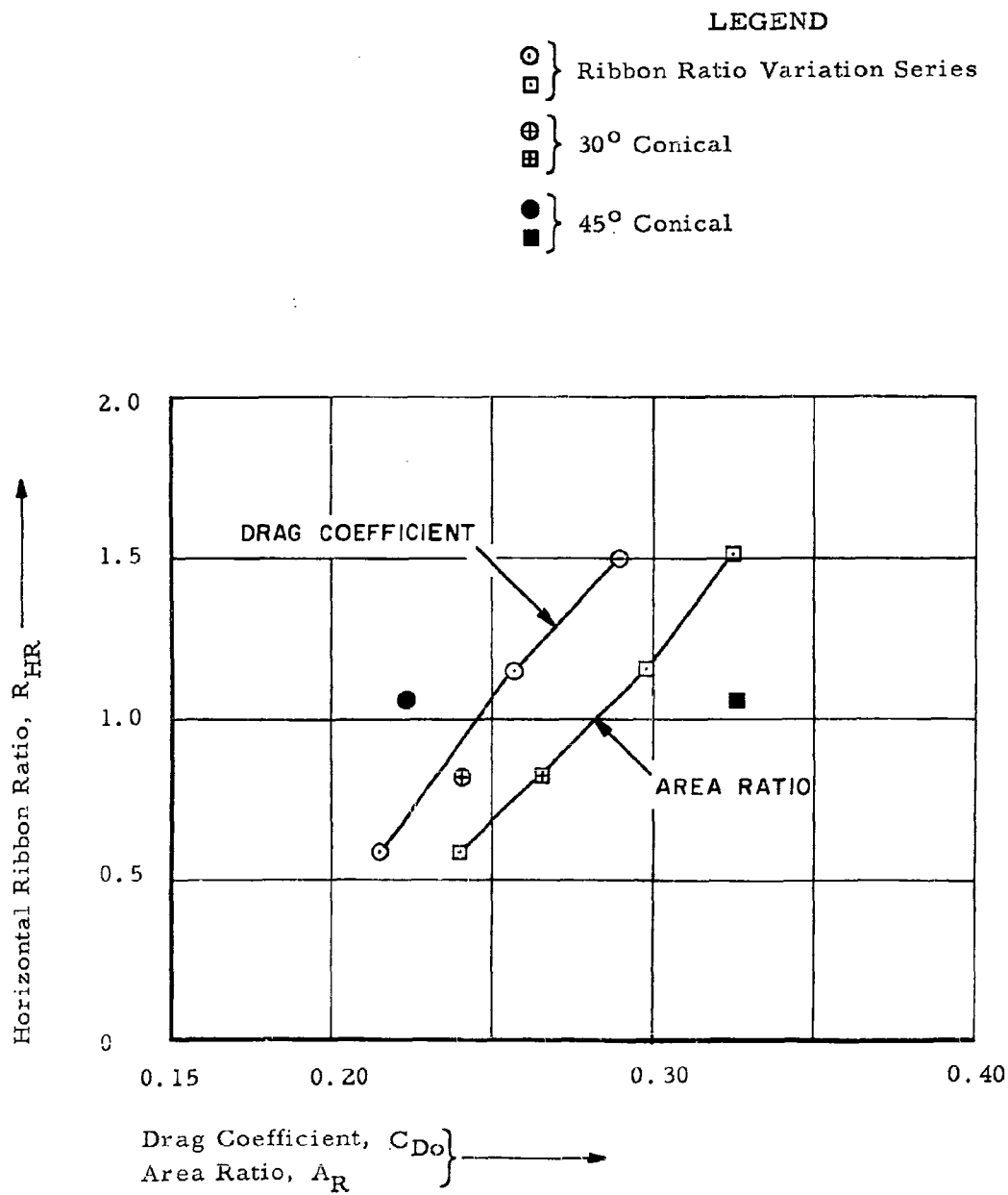


Figure 12. Horizontal Ribbon Ratio vs. Drag Coefficient and Area Ratio for 16 Gore Model Parachutes at Mach 1.9



(a) Porosity = 29.03%
 FIST Ribbon - Space to
 Ribbon Ratio = 1.5
 Film Speed = 2295 F. P. S.
 Dynamic Pressure = 165.96 P. S. F.



(b) Porosity = 24.96%
 FIST Ribbon - Space to
 Ribbon Ratio = 0.586
 Film Speed = 2230 F. P. S.
 Dynamic Pressure = 163.36 P. S. F.

Figure 13. Typical Fabric Parachute Behavior at Mach 1.9

5. Conical Ribbon

Two conical ribbon parachutes were tested to determine the effect of shaped gores and reduced fullness at the canopy skirt. A 30 degree and a 45 degree cone angle were selected. The horizontal ribbon ratio was kept as close to unity as possible and the porosity was maintained in the same range as previous models (28.3 percent). Again the canopies had 16 gores and one diameter suspension lines.

The performance of the conical parachutes was generally better than the flat FIST ribbon type. The 30 degree type was only slightly different than the comparable FIST type and exhibited about the same degree of instability. By contrast the 45 degree canopy demonstrated a marked improvement over the FIST type as far as stability was concerned. Figure 14(a) shows the extreme steadiness of the 45 degree canopy as compared with the 30 degree canopy, Figure 14(b). Note the cone-shaped interline shock wave existing at all times in the case of the 45 degree configuration while in the 30 degree model this shock wave is occasionally swallowed by the parachute canopy. Note that the disappearance of the interline or conical shock wave is accompanied by a reduction in inflated area.

The 45 degree conical ribbon parachute had the highest average inflated area ratio (0.326) of all parachutes tested. It also had the most stable canopy. For some reason, the drag force measured on this test was very low and a value of drag coefficient, 0.224, resulted. The 30 degree conical had an area ratio of only 0.266 and yet attained a drag coefficient of 0.242. When the values of A_R and C_{D0} of the two conical parachutes are plotted in Figure 12 with the other 16 gore canopies, the results are very interesting. The points for the 30 degree conical fall almost perfectly in the pattern established by the standard FIST ribbon parachutes. However, the 45 degree conical shows a serious discrepancy. The area ratio point fell to the right of the regular A_R curve. However, the C_{D0} fell to the left of the C_{D0} curve. This inconsistency, plus the fact that the measured drag force was very low when compared with other similar tests, leads to the conclusion that unreliable force data was obtained on the test involving the 45 degree conical ribbon parachute.

This Document
Reproduced From
Best Available Copy



(a) Porosity 28.3%
Ribbon Ratio = 1.05
45° Conical Ribbon
Film Speed = 2230 F. P. S.
Dynamic Pressure = 160.72 P. S. F.

(b) Porosity = 28.3%
Ribbon Ratio = 0.813
30° Conical Ribbon
Film Speed = 2280 F. P. S.
Dynamic Pressure = 174.36 P. S. F.

Figure 14. Typical Fabric Parachute Behavior at Mach 1.9,
WADC TR 58-284
PART III

E. Discussion of Results

The behavior of the fabric parachute canopies seems to be somewhat dependent upon the location and action of the interline shock wave. Figure 15 shows a number of typical frame enlargements from the Schlieren film of the test runs. In all cases presented there exists an interline conical shock wave. This shock wave shows considerable variation in shape and size between the various tests.

Figure 15(c) is the most typical of the group. Note that the normal shock wave seems to extend across the mouth of the canopy with the interline shock wave superimposed upon the normal shock and extending in front of and out just beyond the canopy skirt.

Figure 15(e) shows two views of the test parachute with the horizontal ribbon ratio of 1.50. Note how the interline shock has moved along one of the suspension lines during this sequence. Also, the apex of the cone of the interline shock is not centered with reference to the canopy mouth. The elapsed time between the two frames is less than 1 millisecond.

In all cases the canopy opens widest when the apex of the interline shock cone is at the farthest forward position. There are some cases where the interline shock is not in evidence, having been completely swallowed by the canopy. Invariably this condition is accompanied by an almost completely collapsed canopy (see Figure 14(b)). If the interline shock wave remains steady then the canopy also becomes steady (see Figure 14(a)). It is possible that the location and behavior of the interline shock is a function of the inflated shape of the parachute canopy rather than vice versa. It is not possible at this time to determine which is cause and which is effect.

However, it seems logical to assume that if the interline shock wave could be controlled and stabilized the result would be a stable canopy. Control of the interline shock wave might be accomplished by a shock generator located a short distance behind the confluence point midway between the suspension lines. It might be possible to mount the shock generator on a central line running from the confluence point to the canopy vent.

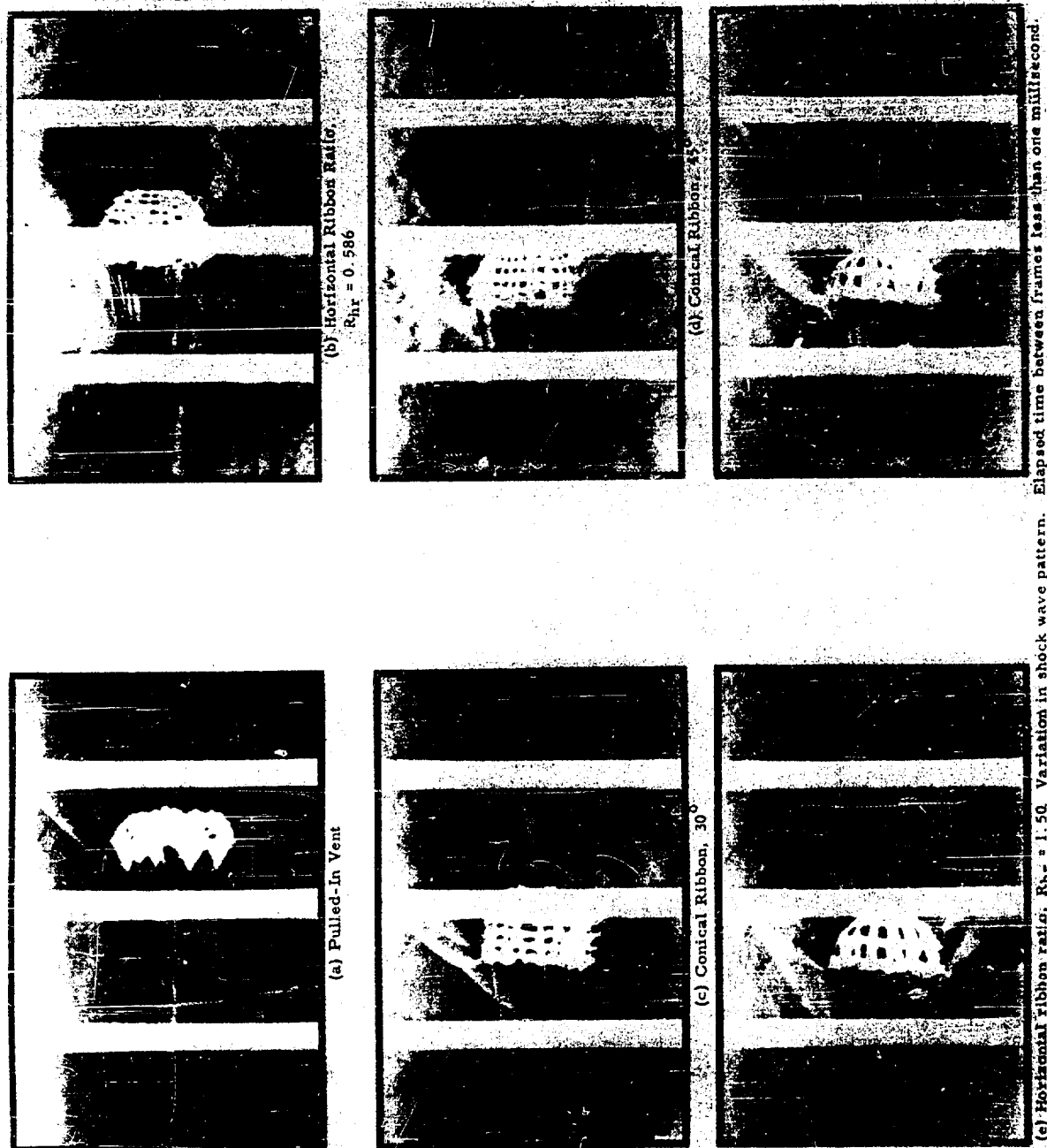


Figure 15. Typical Shock Patterns of Several Fabric Canopies at Mach 1.9

SECTION IV

GENERAL CONCLUSIONS

The previous wind tunnel program, reported in Reference 1, led to a number of conclusions which will be restated here for convenience.

- (1) Fabric canopies did not fully inflate and gave a much-reduced drag coefficient. Violent breathing existed at all Mach numbers.
- (2) Solid metal canopies exhibited unstable flow patterns both with and without suspension lines. The flow patterns of the canopies with lines were very similar to those observed for flexible models. It can then be concluded that the unstable flow was not necessarily caused by the canopy flexibility although it might be a contributing factor.
- (3) The causes of the unstable flow were either interaction between shock fronts or choking of the flow through the canopy.

Attempts to relieve choking by providing the canopies with vents and by increasing porosity in the present program gave the following results:

- (1) Steady flow existed for all tests of canopies without suspension lines. Porosities were varied between 28 and 45 percent and Mach numbers between 1.70 and 3.50.
- (2) Unsteady flow existed for all tests of solid canopies with suspension lines. However, only the 45 percent canopy was tested. The Mach number was varied between 1.70 and 3.50. The number of suspension lines used were either 6, 12 or 24. No improvement was noted with reduction in number of suspension lines.

The fabric canopies tested in the present program gave the following results:

- (1) The flow patterns were somewhat different than for the solid canopies. Instability and canopy breathing was fairly general. An increase in the porosity and the number of gores gave a slightly improved performance. Drag coefficients were low in all cases. The low values of C_{D0} were partially the result of underinflation.

(2) The conical ribbon parachutes appeared to perform the best with the 45 degree behaving better than the 30 degree.

(3) The action of the fabric parachutes was dependent upon the position of the interline shock wave. This shock wave generally took a position midway between the confluence point and the parachute skirt. When flow was steady, the interline shock was a cone (see Figure 14) which blended into the normal shock off the canopy skirt. When unstable flow existed, this shock seemed to propagate along one or more individual suspension lines in the direction of the confluence point. The canopy inflated area would invariably change with change in interline shock wave position. It was not possible to tell which was cause and which was effect.

APPENDIX I

RIGID PARACHUTE MODEL DESIGN

A. General

The rigid model parachutes used in the tests discussed in this report were similar in design to those used in the test program reported in Reference 1. One of the recommendations made in Reference 1 was to include vents in all canopies. It was hoped that the inclusion of such vents would prevent choking of the canopy which would very likely improve parachute behavior.

Accordingly, a new series of solid canopies were designed and fabricated using the shape specifications outlined in Reference 2. Since all of the canopies were provided with vents at the apex of the canopy, the previous sting support could not be used. Therefore, a modified sting which would permit the use of an open vent was designed. This redesigned sting was a yoke type which supported the canopy at four points located approximately midway between the skirt and crown.

Figure 1 shows one of the solid canopies mounted on the special sting support in the wind tunnel. Figure 3 is a close-up of the yoke type sting assembled to a typical rigid canopy.

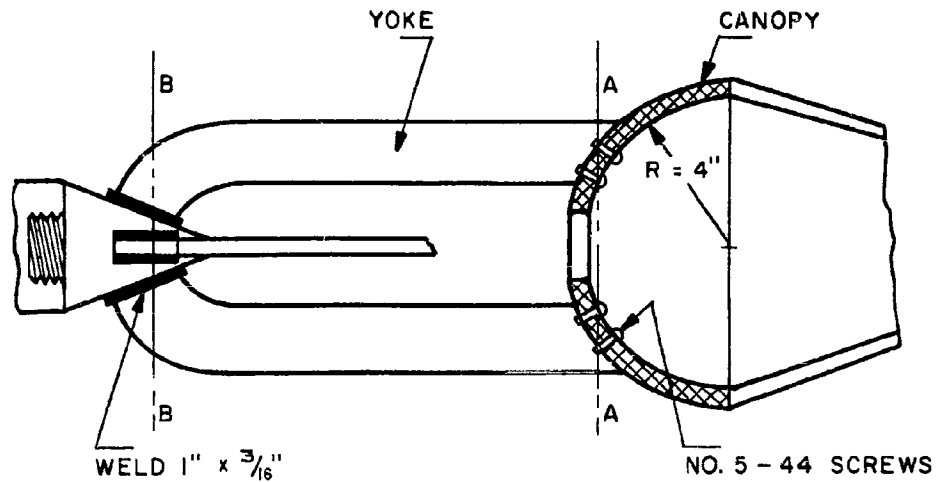
B. Stress Analysis

This section covers the strength analysis of a rigid parachute model under room temperature conditions and assumes a dynamic pressure of 100 lbs/ft². While the entire structure of the model has been thoroughly examined, the following discussion covers only the most critical components.

It is believed that the methods used in this analysis are obvious with the possible exception of the calculation of the discontinuity stresses in the canopy. A complete discussion of the method used to calculate these stresses can be found in Reference 3.

While this analysis was based on a dynamic pressure of 100 lbs/ft², the conservative techniques used in calculating both the stresses and the aerodynamic loads make it possible to test up to a dynamic pressure of 200 lbs/ft² and still maintain an adequate factor of safety.

1. Yoke Support



It was found that the No. 5-44 screws at section A-A and the weld at section B-B were the critical items of the yoke support.

a. Section A-A

At this section there existed a 188 in.-lb moment which the screws absorbed in shear. The magnitude of the shear stress was found from the expression:

$$\tau = \frac{M}{4RA}$$

Where:

τ = shear stress

M = bending moment

R = canopy radius

A = screw area

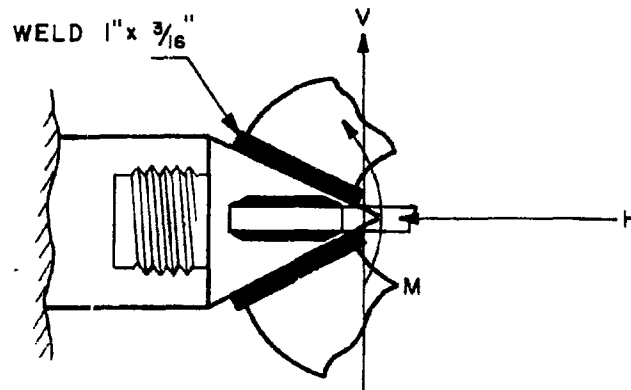
4 = number of screws

CALCULATION:

$$\tau = \frac{188}{4(4)(0.00716)} = 1641 \text{ lbs/in.}^2$$

Safety Factor = Large

b. Section B-B

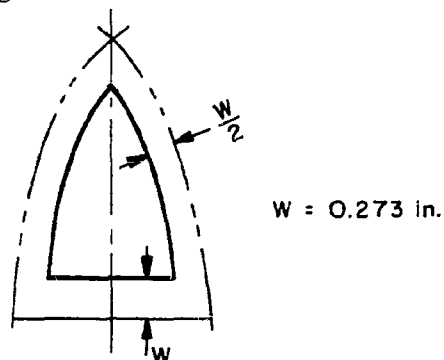


$$\begin{aligned} M &= 423 \text{ in.}-\text{lbs} \\ H &= 33 \text{ lbs} \\ V &= 22 \text{ lbs} \end{aligned}$$

The horizontal and vertical forces were ignored and it was assumed that the moment M would be absorbed by the vertical arms alone. The maximum fiber stress in the weld was found to be 4785 lbs/in.^2 . The weld metal had a minimum yield strength of $60,000 \text{ lbs/in.}^2$ and the yield strength of the parent metal was $52,000 \text{ lbs/in.}^2$. This provided the welds with a safety factor of 10 or better.

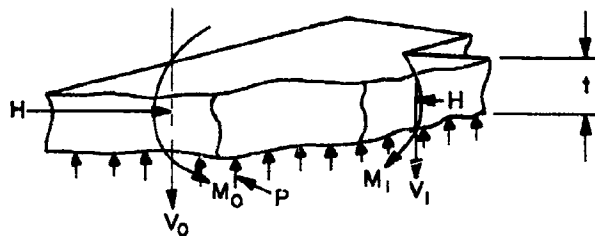
2. Canopy

Of all the canopies considered for testing, the canopy with a gore design as shown below was found to be the most critical from a strength standpoint. This same configuration can be assumed for all canopies if the effects of all horizontal ribbons except at the skirt and the vent are neglected.



CRITICAL GORE CONFIGURATION

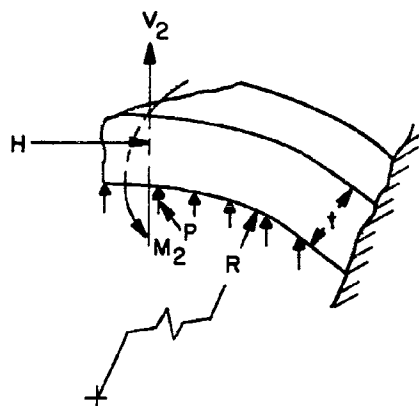
This gore is formed from 24 radial ribbons with only one horizontal ribbon located at the mouth or skirt of the canopy.



$$\begin{aligned} H &= 0.41 \text{ lbs} \\ M_0 &= 4.6 \text{ in.-lbs/in.} \\ V_0 &= 0.67 \text{ lbs/in.} \\ M_1 &= 10.4 \text{ in.-lbs/in.} \\ V_1 &= 4 \text{ lbs/in.} \\ p &= 100 \text{ lbs/ft}^2 \\ t &= 0.093 \text{ in.} \end{aligned}$$

FREE BODY OF THE HORIZONTAL RIBBON

$$\begin{aligned} H &= 0.41 \text{ lbs} \\ M_2 &= 11 \text{ in.-lbs} \\ V_2 &= 4.3 \text{ lbs} \\ p &= 100 \text{ lbs/ft}^2 \\ t &= 0.093 \text{ in.} \\ R &= 4 \text{ in.} \end{aligned}$$



FREE BODY OF THE RADIAL RIBBON

Canopy Material - 302 Stainless Steel
Yield Strength - 80,000 lbs/in.²

The magnitude of the moments and forces shown above were obtained from a consideration of the deflection and rotation of the canopy ribbons and the 24 riser lines. To calculate these quantities the horizontal ribbon was treated as a short cylinder and the radial ribbons were considered as thin curved cantilever beams. The 24 suspension lines were assumed to be simply supported beams with an edge moment at the canopy end of the lines. (See Section 3 below).

a. Radial Ribbons

The horizontal and vertical forces do not significantly influence the stress in these ribbons and can be ignored. The edge moment M_2 developed a bending stress σ_b as follows:

$$\sigma_b = \frac{M_2}{Z}$$

Where:

σ_b = maximum fiber stress

M_2 = edge moments

Z = section modulus

CALCULATION:

$$\sigma_b = \frac{11}{0.0004} = 27,500 \text{ lbs/in.}^2$$

$$\text{Safety Factor} = \frac{80,000}{27,500} = 2.9$$

Ignoring the influence of the suspension lines and the horizontal ribbon, the maximum fiber stress in the radials due to the pressure p is given by:

$$\sigma = p \frac{R}{t} \left(1 + \frac{6R}{t} \right)$$

Where:

σ = maximum normal stress

p = pressure

R = ribbon radius

t = material thickness

CALCULATION:

$$\sigma = 0.694 \left(\frac{4}{0.094} \right) \left[1 + \frac{6(4)}{0.094} \right] = 7,570 \text{ lbs/in.}^2$$

$$\text{Safety Factor} = \frac{80,000}{7,570} = 10.6$$

b. Horizontal Ribbon

Assuming that the horizontal ribbon does not bend or twist, and that each cross section of the ribbon rotates in its own plane about its centroid, the maximum normal stress can be found from the following expression:

$$\sigma = \frac{R}{Z} \left[(V_1 - V_0) \frac{W}{2} + M_1 - M_0 \right] + \frac{R}{Wt} (V_1 - V_0) p \frac{R}{t}$$

Where:

σ = maximum normal stress
 Z = section modulus
 R = ribbon radius
 V_1 & V_0 = edge shear/length
 M_1 & M_0 = edge moment/length
 p = air pressure
 W = ribbon width
 t = ribbon thickness

CALCULATION:

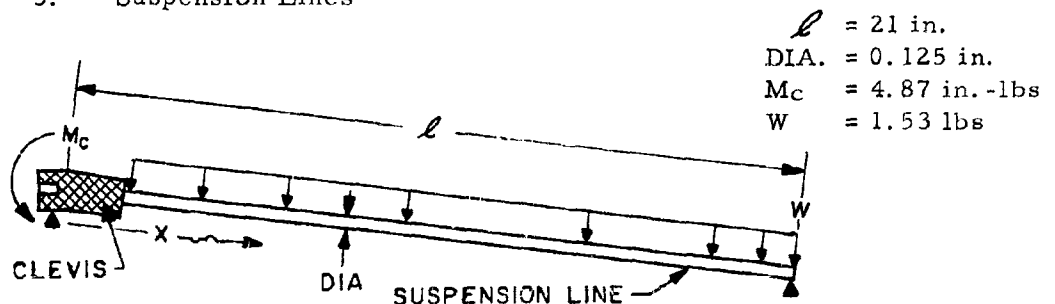
$$\sigma = \frac{4}{0.001164} \left[(4 - 0.67) \frac{0.273}{2} + 10.4 - 4.6 \right]$$

$$= \frac{4(4 - 0.67)}{0.273(0.094)} + \frac{0.694(4)}{0.094}$$

$$\sigma = 22,200 \text{ lbs/in.}^2$$

$$\text{Safety Factor} = \frac{80,000}{22,200} = 3.6$$

3. Suspension Lines



FREE BODY DIAGRAM OF THE SUSPENSION LINES

Riser Line Material - 440-F Stainless Steel
Yield Strength - 100,000 lbs/in.²

The total load W was found by assuming that the pressure distribution along the length of the line was uniform. The edge moment M was obtained by using the technique described in section 2. The maximum bending stress at any section can then be found from the following equation:

$$\sigma_b = \frac{1}{Z} \left[\frac{W}{2} \left(X - \frac{X^2}{\ell} \right) - M_c \left(1 - \frac{X}{\ell} \right) \right]$$

Where:

σ_b = maximum bending stress
Z = section modulus
W = total load
 M_c = end moment from the canopy
 ℓ = total line length
X = distance to any section

CALCULATION:

The maximum stress was found at X = 0.5.

$$\sigma_b = \frac{1}{0.0001918} \left[\frac{1.53}{2} \left(0.5 - \frac{0.25}{21} \right) - 4.87 \left(1 - \frac{0.5}{21} \right) \right]$$

$$b = 21,600 \text{ lbs/in.}^2$$

$$\text{Safety Factor} = \frac{100,000}{21,600} = 4.6$$

APPENDIX II

FABRIC MODEL PARACHUTE DESIGN

A. Introduction

The fabric test model parachutes used on the program were designed on the same basis as the solid canopies. The largest parachute which could be tested in the Langley tunnel was one with an 8-inch inflated diameter. Accordingly, a series of parachutes were designed and constructed to meet with the above requirement.

In order to provide a suitable mount or sting for testing the fabric parachutes it became necessary to design and build a special mount assembly. This mount (see Figure 2) was located upstream from the test section a sufficient distance to permit adequate viewing of the test parachute through the test section windows. Included in the special mount was a deployment mechanism with which it was possible to eject the parachute by remote control at any desired time. Thus, the wind tunnel could be brought up to speed before deploying the parachute.

B. Parachute Design

It is desirable in conducting a wind-tunnel test program to utilize test models which are as close as possible in size to the actual unit. The 4x4 ft Langley tunnel will permit testing of a model with a maximum diameter of approximately 8 inches. Test model parachutes were therefore designed which would, when fully inflated, not exceed such a size. Normally, a parachute will inflate to a diameter which is two-thirds of its constructed diameter. Thus an 8-inch inflated diameter would be produced by a parachute that had a 12-inch constructed diameter.

All of the test parachutes designed for this series of tests were made 12 inches in diameter or as close to this dimension as possible while still satisfying all of the other design parameters involved. In the case of the three parachute cluster, the total inflated area was made equal to the area of an 8-inch diameter circle.

The first five tests were performed with parachutes having only 8 gores while the remainder involved parachutes with 16 gores. The 16 gore arrangement was preferred and parachutes with a smaller number of gores were used only because it eased the fabrication problem. In all cases suspension lines equal to one parachute diameter were used.

The design of parachutes as small as 12 inches in diameter is somewhat handicapped by the scarcity of suitable materials. The smallest ribbon material which was on hand at the time of development of these test items was 3/8-inch wide. Such a width ribbon would be comparable with a 3/4-inch wide ribbon in a 2 foot diameter parachute and a 1-1/2-inch width in a 4 foot diameter parachute. These widths are reasonably compatible with what has actually been used on full sized test parachutes during the free-flight phases of the study program.

On the 8 gore models where vertical ribbons were used, it became necessary to fold and stitch 3/8-inch wide ribbon to reduce it to 3/16-inch width. A typical gore layout for an 8 gore parachute is shown in Figure 16.

The fabric test model used on Test No. 5 was identical to that used on Test No. 3 with the exception that a single central suspension line was added. This central line was of such a length that when the canopy was fully inflated the crown was held in to about one-half the normal inflated depth. The resulting inflated shape looked somewhat like one-half of a fat doughnut.

The models used on Test Nos. 6, 7, and 8 were standard FIST ribbon types wherein the ratio of the space between horizontal ribbons to the width of the ribbon was varied between 0.586 and 1.50. These parachutes all had 16 gores and a typical gore layout is presented in Figure 17. The last two models were conical ribbon types, one having a cone angle of 30° and the other 45°.

Table 4 presents the physical details and dimensions of all of the test model parachutes.

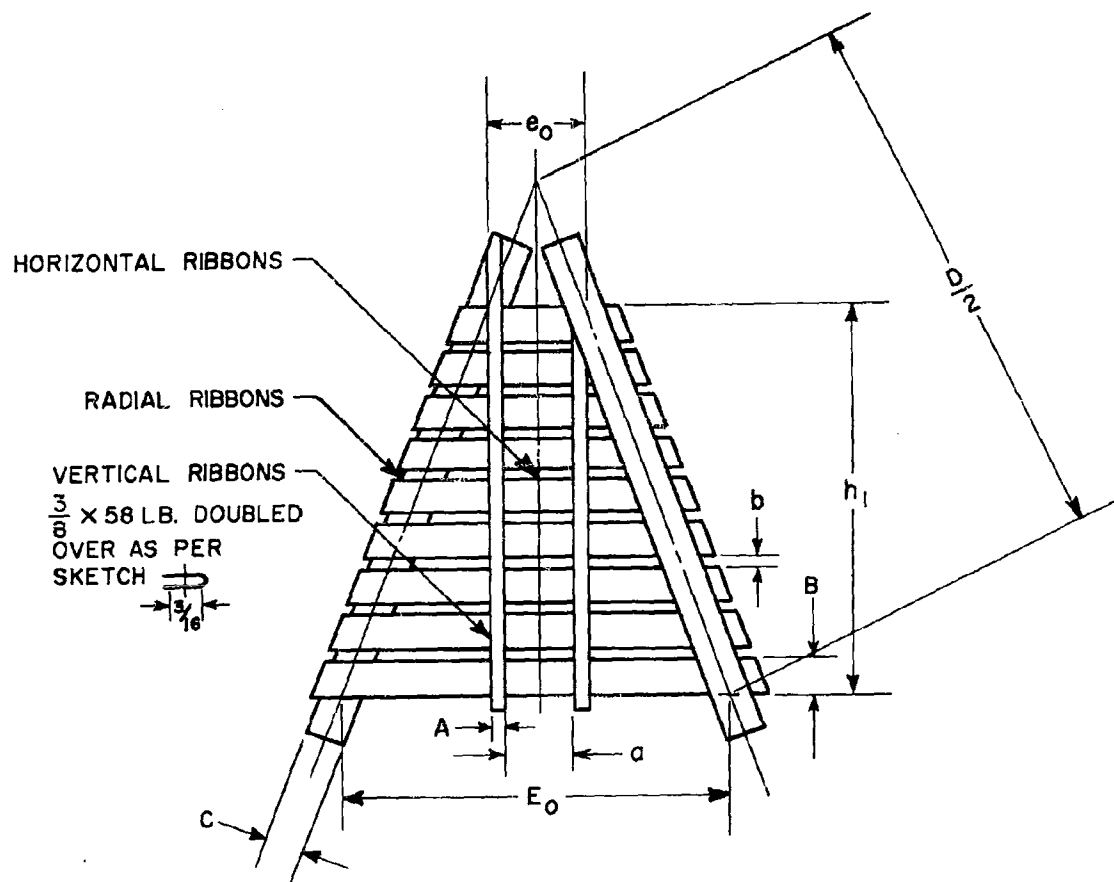


Figure 16. Typical Gore Layout for 8 Gore
FIST Ribbon Parachutes

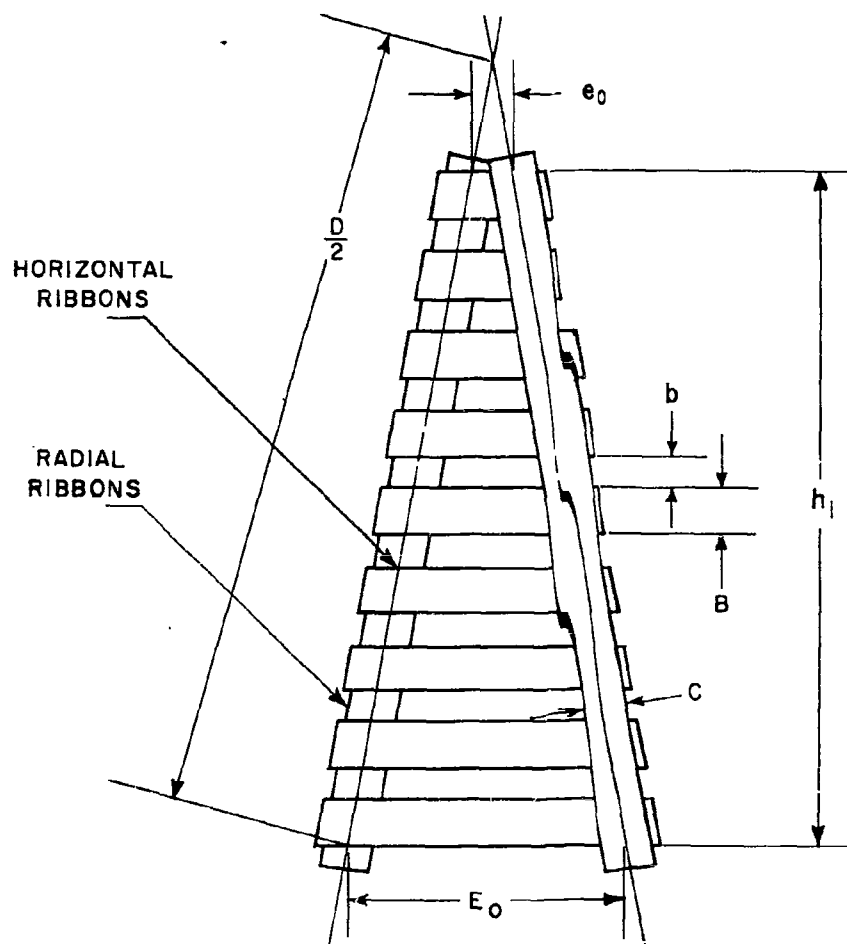


Figure 17. Typical Gore Layout for 16 Gore FIST and Conical Ribbon P parachutes

TABLE 4
PHYSICAL DETAILS OF FABRIC MODEL PARACHUTES

Parachute Number	780	779	777	781	778	17882	17909	17881	17911	17800
Parachute Assembly No.	597-8466	597-8465	597-8464	-	597-8464	597-8862	597-8863	597-8861	597-8865	597-8864
Cord Assembly No.	597-8469	597-8468	597-8467	-	597-8467	597-8867	597-8868	597-8866	597-8854	597-8853
Parachute Type	FIST	FIST	FIST	FIST (1)	FIST (2)	FIST	FIST	FIST	45° conical	30° conical
Used on Test No.	1	2	3	4	5	6	7	8	9	10
Nominal Diameter, D_0 , (in.)	11.4	11.4	11.4	6.15	11.4	9.89	11.9	11.1	9.77	11.09
Nominal Area, S_0 , in ²	102	102	102	29.8	102	72	111.5	96.8	75	96.7
Number of Cores	8	8	8	8	8	16	16	15	16	15
Geometric Porosity, λ g, %	40.5	53.3	20.0	20.0	20.0	29.03	24.96	28.5	28.3	28.3
Vent Porosity, λ v, %	24.0	15.0	1.0	1.0	1.0	1.0	1.0	1.0	1.0	1.0
Horizontal Ribbon Width, B , (in.)	0.375	0.375	0.375	0.375	0.375	0.500	0.375	0.500	0.375	0.375
Horizontal Ribbon Strength, (lb)	58	58	58	58	58	250	58	250	58	58
Number of Horizontal Ribbons	5	6	9	5	9	4	9	5	7	8
Vertical Ribbon Width, A , (in.)	0.187 (0.375 folded)	0.187 (0.375 folded)	0.187 (0.375 folded)	0.085	0.187 (0.375 folded)	-	-	-	-	-
Vertical Ribbon Strength, (lb)	58	58	58	100 lb cord	58	-	-	-	-	-
Number of Vertical Ribbons (per gore)	2	2	2	2	2	-	-	-	-	-
Radial Ribbon Width, C , (in.)	0.375	0.375	0.375	0.375	0.375	0.500	0.375	0.500	0.375	0.375
Radial Ribbon Strength, (lb)	58	58	58	58	58	250	58	250	58	58
Suspension Lines	100 lb cord	100 lb cord	100 lb cord	100 lb cord	100 lb cord	100 lb cord	100 lb cord	100 lb cord	100 lb cord	100 lb cord
Horizontal Ribbon Spacing, b , (in.)	0.19	0.19	0.19	0.23	0.19	0.75	0.22	0.57	0.394	0.305
Horizontal Ribbon Ratio, $b/B = RHR$	0.507	0.507	0.507	0.615	0.507	1.50	0.566	1.145	1.05	0.813
Vertical Ribbon Spacing, a , (in.)	0.75	0.75	0.75	0.75	0.75	-	-	-	-	-
Width of Gore at Skirt, g , (in.)	4.60	4.60	4.60	2.55	4.60	1.95	2.34	2.19	1.61	2.03
Width of Gore at Vent, g_v , (in.)	2.45	2.00	0.59	0.448/0.398	0.59	0.291/0.259	0.335/0.298	0.336/0.282	0.252/0.224	0.300/0.266
Length of Gore, h , (in.)	2.64	3.20	4.90	2.80	4.90	4.25	5.14	4.78	4.99	5.14

(1) Cluster of three (2) Padded-in Crown (3) With Fullness/Actual

APPENDIX III

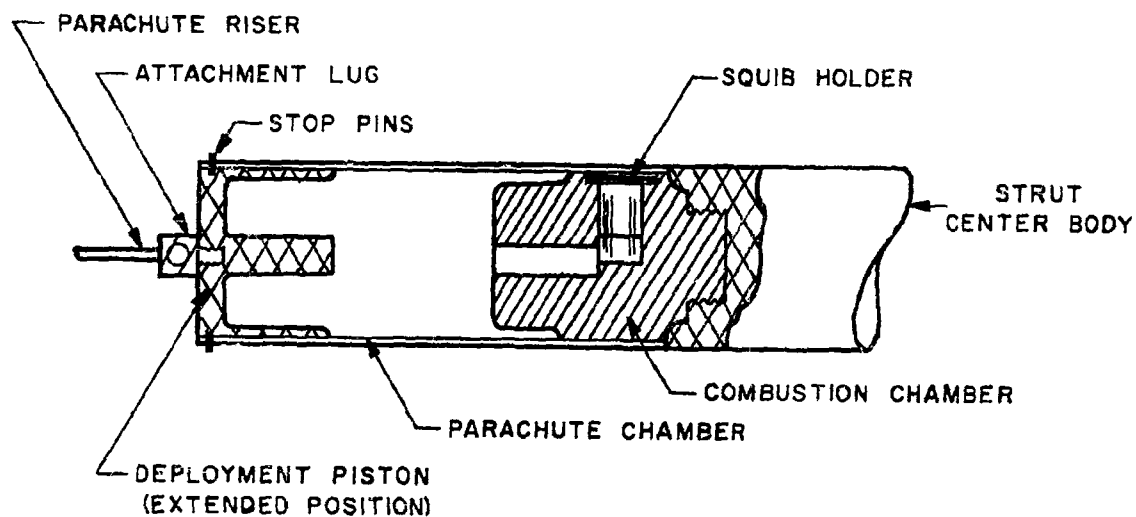
STRESS ANALYSIS OF THE FABRIC PARACHUTE MOUNTING AND DEPLOYMENT SYSTEM

A. General

This analysis covers the strength of a mounting and deployment system for model fabric parachutes. This structure was examined under room temperature conditions with a 200 pound load directed at an angle of 45 degrees with respect to its longitudinal axis.

The basic design of the supporting struts was done by the NASA facility at Langley Field, Virginia. The deployment system was designed by the Cook Research Laboratories.

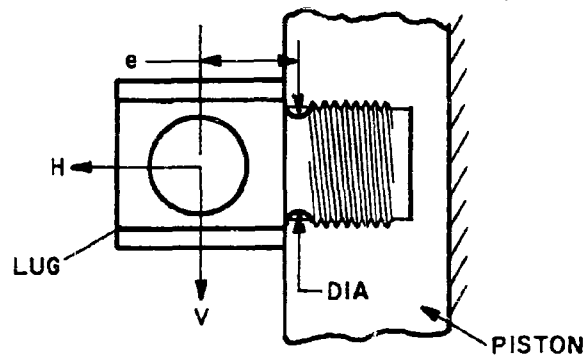
B. Deployment Mechanism



SCHEMATIC DIAGRAM OF THE DEPLOYMENT MECHANISM

The deployment mechanism consisted of a 2-inch diameter body mounted in the center of the tunnel at the junction of the two support struts. The body was essentially a cylinder with a piston actuated by a 1/2 grain squib. The motion of the piston forced the parachute out of the end of the cylinder into the airstream. A tension link was attached to the end of the piston for load measuring purposes.

1. Attachment Lug



H = 140 lb
V = 140 lb
Dia = 0.435 in.
e = 0.25 in.

FREE BODY DIAGRAM OF THE ATTACHMENT LUG

Lug material - 302 stainless steel
Yield strength - 30,000 lb/in.²

The undercut section adjacent to the threads was found to be the critical section of the lug. By ignoring the interaction of the piston and lug, the stress developed can be found from the following expression.

$$\sigma_m = \frac{H}{A} + \frac{Ve}{Z}$$

Where:

σ_m = maximum fiber stress

Ve = bending moment of the vertical load V

e = eccentricity of the load V with respect to the neck of the lug

H = horizontal load

A = cross sectional area

Z = section modulus

CALCULATION:

$$\sigma_m = \frac{140}{0.149} + \frac{140 (0.25)}{0.00806} = 5,280 \text{ lb/in.}^2$$

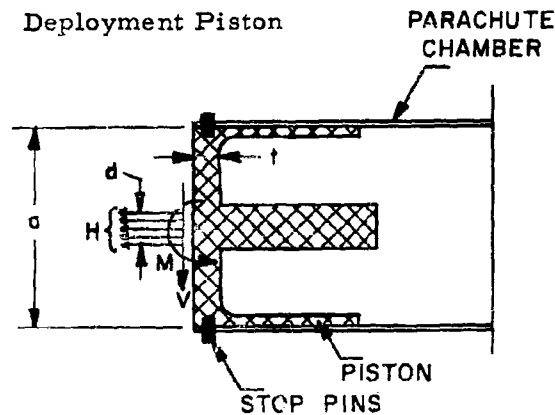
The shear stress developed by the vertical load V is very small and can be ignored. The safety factor of the lug is then

WADC TR 58-284

PART III

$$\text{Safety Factor} = \frac{30,000}{5,280} = 5.6$$

2. Deployment Piston



$$\begin{aligned} H &= 140 \text{ lb} \\ V &= 140 \text{ lb} \\ M &= 35 \text{ in.-lb} \\ a &= 2.125 \\ d &= 0.468 \\ t &= 0.250 \end{aligned}$$

FREE BODY DIAGRAM OF THE DEPLOYMENT PISTON

Piston Material - Naval Brass
Yield Strength - 37,000 lb/in.²

The parachute load is transferred from the center of the piston into the stop pins and then to the parachute chamber. The resulting stress distribution is very complex and difficult to analyze. Therefore, the strength of the piston was checked through actual tests. A first approximation of the required wall thickness t was found by considering the piston as fixed at the center with a concentrated load at an outer edge. By using case 63 on page 211 of Reference 4, an expression for t was found.

$$t = \sqrt{\beta/\sigma \left(\frac{H}{2} + \frac{M}{a} \right)}$$

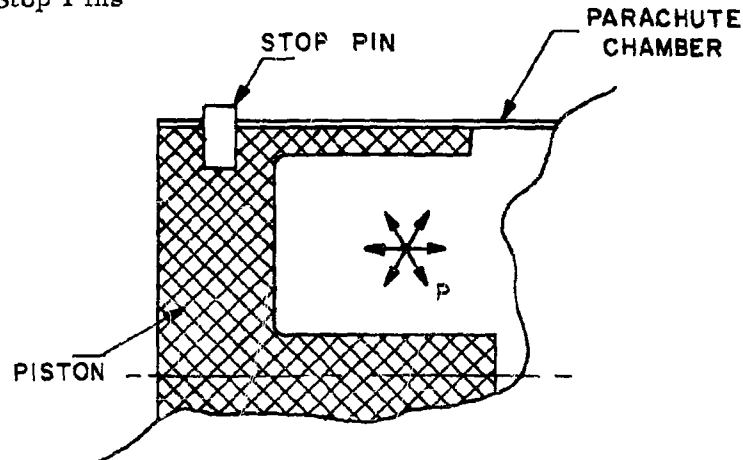
Where:

t = piston wall thickness
 β = coefficient which considers the geometry and elastic properties of the material
 H = horizontal load
 M = bending moment
 a = plate diameter
 σ = material yield strength

CALCULATION:

$$t = \sqrt{\frac{8.4}{37,000} \left(\frac{140}{2} \frac{35}{2.125} \right)} = 0.14 \text{ in.}$$

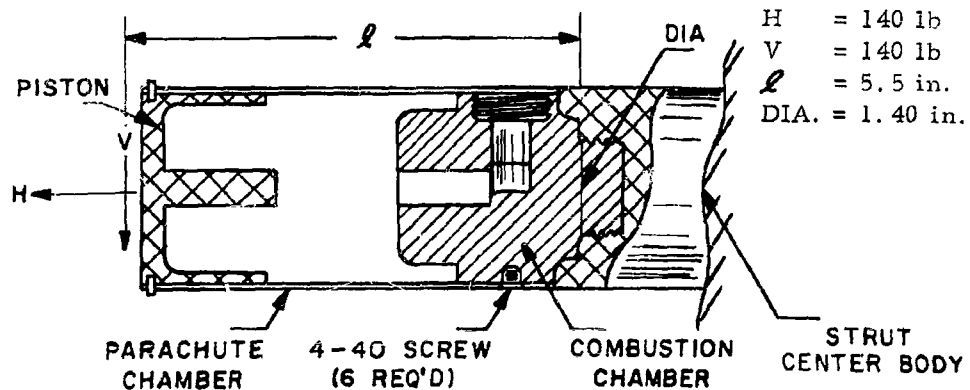
3. Stop Pins



Material - Steel Roll Pin
Double Shear Strength - 4,400 lb

Stop pin loads become critical when arresting the piston after it has been ejected from the combustion chamber. The size of the pin was determined by actual tests

4. Combustion Chamber



FREE BODY DIAGRAM OF THE COMBUSTION CHAMBER

Material - 320 Stainless Steel
Yield Strength - 30,000 lb/in.²

The undercut section adjacent to the threads represented the critical section of the combustion chamber. By ignoring the interaction between the center body and the combustion chamber the maximum fiber stress will be

$$\sigma_m = \frac{H}{A} + \frac{Vl}{Z}$$

Where:

σ_m = maximum fiber stress
H = horizontal load
V = vertical load
l = moment arm of the vertical load
A = cross sectional area
Z = section modulus

CALCULATION:

$$\sigma_m = \frac{140}{1.02} + \frac{140 (5.5)}{0.1454} = 5,440 \text{ lb/in.}^2$$

$$\text{Safety Factor} = \frac{30,000}{5,440} = 5.5$$

5. Parachute Chamber

The maximum fiber stress is obtained from an analysis identical to that used for the combustion chamber. The loads remain the same but the moment arm changes to 3.125 in. and the section modulus becomes 0.0339 in.³. The resulting stress will be 13,250 lb/in.². Considering that this component is made from AISI 4130 steel with a yield strength of 120,000 lb/in.² the safety factor will be large.

REFERENCES

1. Meyer, R. A., Wind Tunnel Investigation of Conventional Types of Parachute Canopies in Supersonic Flow, WADC TR 58-532, Cook Research Laboratories, A Division of Cook Electric Company, December 1958.
2. Topping, A. D., Marketos, I. D., and Costakos, N. C., A Study of Canopy Shapes and Stresses for Parachutes in Steady Descent, WADC Technical Report 55-294, Goodyear Aircraft Corporation, Akron, Ohio October 1955.
3. Timoshenko, S., Advanced Strength of Materials, Vol. II, McGraw-Hill Book Company, Inc., New York, New York.
4. Roark, R. J., Formulas for Stress and Strain, McGraw-Hill Book Company, Inc., New York, New York.